Reduced growth with increased quotas of particulate organic and inorganic carbon in the coccolithophore *Emiliania huxleyi* under future ocean climate change conditions

Yong Zhang[1,4], Sinéad Collins[2], and Kunshan Gao[1,3]

[1]State Key Laboratory of Marine Environmental Science and College of Ocean and Earth Sciences, Xiamen University, Xiamen, China

[2]Institute of Evolutionary Biology, School of Biological Sciences, University of Edinburgh, Edinburgh EH9 3FL, United Kingdom

[3]Co-Innovation Center of Jiangsu Marine Bio-industry Technology, Jiangsu Ocean University, Lianyungang, China

[4]College of Environmental Science and Engineering, and Fujian Key Laboratory of Pollution Control and Resource Recycling, Fujian Normal University, Fuzhou, China

Running head: Response of *E. huxleyi* to multiple drivers

Correspondence: Kunshan Gao (ksgao@xmu.edu.cn)

Keywords: CO_2; coccolithophore; functional trait plasticity; light; multiple drivers; nutrients; ocean acidification; warming.

Abstract

Effects of ocean acidification and warming on marine primary producers can be modulated by other environmental factors, such as levels of nutrients and light. Here, we investigated the interactive effects of five oceanic environmental drivers (CO_2, temperature, light, dissolved inorganic nitrogen and phosphate) on growth rate, particulate organic (POC) and inorganic (PIC) carbon quotas of the cosmopolitan coccolithophore *Emiliania huxleyi*. Population growth rate increased with increasing temperature (16 to 20 °C) and light intensities (60 to 240 µmol photons m^{-2} s^{-1}), but decreased with elevated pCO_2 concentrations (370 to 960 µatm) and reduced availability of nitrate (24.3 to 7.8 µmol L^{-1}) and phosphate (1.5 to 0.5 µmol L^{-1}). POC quotas were predominantly enhanced by combined effects of increased pCO_2 and decreased availability of phosphate. PIC quotas increased with decreased availability of nitrate and phosphate. Our results show that concurrent changes in nutrient concentrations and pCO_2 levels predominantly affected growth, photosynthetic carbon fixation and calcification of *E. huxleyi*, and imply that plastic responses to progressive ocean acidification, warming and decreasing availability of nitrate and phosphate reduce population growth rate while increasing cellular quotas of particulate organic and inorganic carbon of *E. huxleyi*, ultimately affecting coccolithophore-related ecological and biogeochemical processes.

1 Introduction

Ocean acidification (OA), due to continuous oceanic absorption of anthropogenic CO_2, is occurring alongside ocean warming. This in turn, leads to shoaling in the upper mixed layer (UML) and a consequent reduction in the upward transport of nutrients into the UML. These ocean changes expose phytoplankton cells within the UML to multiple simultaneous stressors or drivers, and organismal responses to these drivers can affect both trophic and biogeochemical roles of phytoplankton (see reviews by Boyd et al., 2015; Gao et al., 2019 and literatures therein). While most studies on the effects of ocean global climate changes on marine primary producers have focused on organismal responses to one, two or three environmental drivers, there is an increasing awareness of the need to measure the combined effects of multiple drivers (see reviews by Riebesell and Gattuso, 2015; Boyd et al., 2018; Gao et al., 2019; Kwiatkowski et al., 2019). For this purpose, several manipulative experimental approaches have been recommended (Boyd et al., 2018). One approach using many unique combinations of different numbers of drivers showed that both short and long-term growth responses were, on average, explained by the dominant single driver in a multi-driver environment, but this result relies on having many (>5) drivers with known or measured large-effect single drivers (Brennan and Collins, 2015; Brennan et al., 2017). For experiments with multiple drivers where interactions are likely to preclude making predictions from single drivers, where average responses are not the most informative ones, or where logistics preclude using a very large number of multi-driver environments, Boyd et al. (2010) suggested an 'environmental cluster' method where key drivers (such as temperature, light intensity, nutrient concentration, CO_2 and Fe) are covaried within experiments, allowing the investigation of physiological responses of phytoplankton to concurrent changes of the clustered

drivers. This approach examines responses to projected overall environmental shifts rather than pulling apart the biological or statistical interactions between responses to individual drivers. To our knowledge, studies to date have employed such a driver clustering approach to investigate responses of diatoms *Fragilariopsis cylindrus*, *Thalassiosira pseudonana*, *Skeletonema costatum*, and the prymnesiophyte *Phaeocystis antarctica* to combinations of drivers projected for 2100 (Xu et al., 2014a; Xu et al., 2014b; Boyd et al., 2016).

An environmental cluster approach is especially useful when drivers are known to interact in terms of the organismal responses they elicit, as is the case for OA, light levels, and key nutrients acting on population growth rate and carbon fixation (Boyd et al., 2016). For example, in the cosmopolitan coccolithophore *Emiliania huxleyi*, interactive effects of OA and light showed that OA increased population growth rate and photosynthetic carbon fixation under low light, whereas it slightly lowered population growth rate and photosynthetic carbon fixation under high light (Zondervan et al., 2002; Kottmeier et al., 2016). In addition, photosynthetic carbon fixation was further enhanced by longer light exposure at high pCO_2 levels (Zondervan et al., 2002). On the other hand, OA can exacerbate the negative impact of solar UV radiation on photosynthetic carbon fixation and calcification in *E. huxleyi* under nutrient-replete conditions (Gao et al., 2009), but can increase calcification (coccolith volume) and particulate organic carbon (POC) quota under phosphate-limited conditions (Leonardos and Geider, 2005; Müller et al., 2017), demonstrating that the effects of OA on calcification is likely nutrient-dependent. On the other hand, ocean warming, which occurs alongside OA, is known to increase coccolith length, POC, particulate organic nitrogen (PON) and inorganic carbon (PIC) production rates of several *E. huxleyi* strains (Rosas-Navarro et al., 2016; Feng et al., 2017). Warming

has also been shown to increase the optimal pCO_2 levels for growth, POC and PIC production rates (Sett et al., 2014). In one case warming was found to compensate for the negative impact of OA on growth rate under low light intensity (Feng et al., 2008). Nevertheless, decreased photosynthetic carbon fixation and calcification at reduced carbonate saturation state (lowered Ca^{2+} concentrations) were exacerbated by warming treatment (Xu et al., 2011). Overall, there is strong evidence that understanding the plastic responses of this key calcifier to ocean changes requires investigating responses to the overall expected shift in the environment, in addition to the detailed studies to date on individual drivers, due to the sheer number of interactions between individual drivers on traits that affect the trophic and biogeochemical roles of *E. huxleyi.*

Despite known interactions among two- and three-way combinations of OA, temperature, light, phosphate levels and nitrogen levels, there have been few empirical studies investigating effects of the larger cluster projected for future surface ocean changes. The data to date show that interactions among drivers can affect both the direction and magnitude of trait changes in biogeochemically important taxa. In addition, based on single or two-driver studies, changes in temperature, pCO_2, light, dissolved inorganic nitrogen (DIN) and phosphate (DIP) in combination are predicted to affect primary productions (Barton et al., 2016; Monteiro et al., 2016; Boyd et al., 2018; Gao et al., 2019; Kwiatkowski et al., 2019). Understanding the trait-based responses of cocolithophores to future ocean changes is important for projections of changes in the biogeochemical roles of phytoplankton, such as biological carbon pump efficiency (Rost and Riebesell, 2004).

In order to understand the combined effects of pCO_2, temperature, light, dissolved inorganic nitrogen (DIN) and phosphate (DIP) on functional traits, we incubated

Emiliania huxleyi (Lohmann) under different combinations of environmental conditions that represented subsets of, and eventually the complete set of environments for, this environmental driver cluster. We recently examined the interactive effects of light intensity and CO_2 level on growth rate, POC and PIC quotas of *E. huxleyi* under nutrients replete, low DIN, or low DIP concentrations (Zhang et al., 2019). Light, CO_2, DIN and DIP levels usually change simultaneously with temperature, and temperature modulated responses of *E. huxleyi* to other environmental drivers (Gafar and Schulz, 2018; Tong et al., 2019). In addition, warming or cooling can direcly influence the activity of enzymes, thus directly modulating metabolic rates (Sett et al., 2014). Because of the overwhelming evidence that temperature can act as a general modulator of organismal responses, we use the present study to examine how the addition of temperature as a key driver in the environmental change cluster can modulate the combined effects of CO_2, light and nutrients. We found that future ocean scenario treatments with OA, warming, increased light and reduced availability of nutrients led to lower growth rate and larger POC and PIC quotas of *E. huxleyi*.

2 Materials and Methods

2.1 Experimental setup

Emiliania huxleyi strain PML B92/11 was originally isolated from coastal waters off Bergen, Norway, and obtained from the Plymouth algal culture collection, UK. The average levels of pCO_2, temperature, light, dissolved inorganic nitrate (DIN) and phosphate (DIP) were set up according to recorded data in Norwegian coastal waters during 2000 to 2007 and projected for 2100 in high-latitudes (Larsen et al., 2004; Locarnini et al., 2006; Omar et al., 2010; Boyd et al., 2015) (Table S1). *E. huxleyi* was

cultured with a 12 h/12 h light/dark cycle in thermo-controlled incubators in Aquil medium, which was prepared according to Sunda et al. (2005) with the addition of 2200 μmol L^{-1} bicarbonate to achieve the total alkalinity (TA) of 2200 μmol L^{-1}. Initial DIN and DIP concentrations were 24 μmol L^{-1} and 1.5 μmol L^{-1}, respectively, and initial light intensity was 60 μmol photons m^{-2} s^{-1}. The experiment was conducted in five steps (Fig. 1). Considering ocean acidification and warming as the key drivers for ocean climate changes, we first established 4 "baseline" treatments where the pCO_2 and temperature drivers were combined in a fully factorial way: low pCO_2 + low temperature (LCLT), high pCO_2 + low temperature (HCLT), low pCO_2 + high temperature (LCHT), and high pCO_2 + high temperature (HCHT). Since reduced availability of nutrients and increased light exposures are triggered by warming-enhanced stratification, we then added additional single or pairs of drivers to each of these "baseline" treatments (Fig. S1). In step 1, low light (LL, 60 μmol photons m^{-2} s^{-1}) was supplied; in step 2, high light (HL, 240 μmol photons m^{-2} s^{-1}) was exposed. HL was then maintained for the rest of the experiment. In step 3, low nitrogen was supplied and high phosphate levels were maintained (LNHP). In step 4, low phosphate was supplied and high nitrogen levels were restored (HNLP). In step 5, both nitrogen and phosphate were low (LNLP), respectively (Figs. 1 and S1). In all cases, the cells were acclimated to each unique stressor cluster for at least 14–16 generations before physiological and biochemical parameters were measured. Although this stepwise design introduces a historical effect, physiological traits are generally reported after 10 to 20 generations acclimation to OA treatment (Perrin et al., 2016; Tong et al., 2016; Li et al., 2017), so the historical effects here are similar to those that would be introduced with standard methods in other physiology studies (Tong et al., 2016; Zhang et al., 2019). Since individually reduced availability of

nitrate or phosphate decreased growth, did not change POC quota, and enhanced PIC quota under optimal light intensity (HL in this study) in the same *E. huxleyi* strain (Zhang et al., 2019), we hypothesized that combination of DIN and DIP limitation would result in similar trend under the pCO_2 and/or temperature combined treatments. Therefore, we added stepwise nitrate and/or phosphate drivers (Fig. 1). Such stepwise reduction of nutrients levels would be useful for us to analyze effects of nitrate and phosphate separately, and be expected to have implications for the cells episodically exposed to different levels of nutrients in the sea.

For step 1, NO_3^- and PO_4^{3-} were modified to 24 μmol L^{-1} and 1.5 μmol L^{-1}, respectively, which is the HNHP treatment in the synthetic seawater (Sunda et al., 2005) (Fig. S1). The seawater was dispensed into 4 glass bottles, and 2 bottles of seawater were placed at 16 °C (LT) in an incubator (HP400G-XZ, Ruihua, Wuhan), and aerated for 24 h with filtered (PVDF 0.22 μm pore size, Haining) air containing 400 μatm (LC) or 1000 μatm pCO_2 (HC). Another 2 bottles of seawater were maintained at 20 °C (HT) in the other chamber and also aerated with LC or HC air as described above. The dry air/CO_2 mixture was humidified with deionized water prior to the aeration to minimize evaporation. The LCLT, HCLT, LCHT and HCHT seawaters (Figs. 1a and S1) were then filtered (0.22 μm pore size, Polycap 75 AS, Whatman) and carefully pumped into autoclaved 250 mL polycarbonate bottles (Nalgene, 4 replicate flasks for each of LCLT, HCLT, LCHT and HCHT, a total of 16 flasks at the beginning of the experiment) with no headspace to minimize gas exchange. The flasks were inoculated at a cell density of about 150 cells mL^{-1}. The volume of the inoculum was calculated (see below) and the same volume of seawater was taken out from the bottles before inoculation. The samples were initially cultured at 60 μmol photons m^{-2} s^{-1} (LL) of photosynthetically active radiation (PAR)

(measured using a PAR Detector, PMA 2132 from Solar Light Company) under LCLT, HCLT, LCHT and HCHT conditions for 8 generations (6 days) (d), and then the samples were diluted to their initial concentrations and grown for another 8 generations (6 d) (Fig. 1a). Samples in culture bottles were mixed twice a day at 9:00 a.m. and 5:00 p.m. At the end of the incubation, sub-samples were taken for measurements of cell concentration, POC and TPC quotas, TA, pH and nutrient concentrations.

In step 2, samples grown under the previous conditions were transferred at the end of the cultures from 60 (LL) to 240 μmol photons m^{-2} s^{-1} (HL) of PAR with initial cell concentrations of 150 cells mL^{-1}, and acclimated to the HL for 8 generations (5 d in 16 °C environment, 4 d in 20 °C environment) (Fig. 1b). The cultures were then diluted to achieve initial cell concentration and incubated at the HL for another 8 generations (the fifth day in 16 °C environment and the fourth day in 20 °C environment) before sub-samples were taken for measurements.

In step 3, step 4 and step 5, NO_3^- and PO_4^{3-} concentrations were set to be 8 μmol L^{-1} and 1.5 μmol L^{-1} for the LNHP treatment, and 24 μmol L^{-1} and 0.5 μmol L^{-1} for the HNLP treatment, and 8 μmol L^{-1} and 0.5 μmol L^{-1} for the LNLP treatment, respectively (Fig. 1c,d,e). The LCLT, HCLT, LCHT and HCHT were step 1 conditions, now we are into step 3, 4 and 5. Under 240 μmol photons m^{-2} s^{-1} (HL) of PAR, cell samples with an initial concentration of 150 cells mL^{-1} were transferred from HNHP condition (step 2) to LNHP conditions (step 3) and acclimated to LNHP conditions for 8 generations (5 d in 16 °C environment, 4 d in 20 °C environment) (Fig. 1c). The cultures were then diluted back to initial cell concentrations and incubated in the LNHP conditions (step 3) for a further 8 generations. On the last day

of the incubation (the fifth day in 16 ºC environment and the fourth day in 20 ºC environment), sub-samples were taken for measurements of the parameters.

After that, cell samples were transferred stepwise from HNHP conditions (step 2, Fig. 1b) to HNLP conditions (step 4, Fig. 1d), then from HNLP conditions to LNLP conditions (step 5, Fig. 1e). Cell samples were acclimated for 8 generations at HNLP and LNLP conditions, respectively, and followed by another 8 generation incubations for 4 d at HT and 5 d at LT. On the fourth day (for populations in high temperature environments) or the fifth day (for populations in low temperature environments), sub-samples were taken for measurements (Fig. 1d,e). At low nutrient concentrations, maximal cell concentrations were limited by nutrients (Rouco et al., 2013; Rokitta et al., 2016). To check whether cells sampled were in exponential growth at each nutrient level, we examined cell concentrations every day at LCHT, or LCLT and high light conditions (Fig. S2). We found that cell concentrations were in the exponential growth phase during the 1^{st} and 5^{th} days at HT, and during the 1^{st} and 7^{th} days at LT. In this study, we took samples in the 4^{th} day at HT and in the 5^{th} day at LT, and thus cells sampled were in the exponential growth phase of *E. huxleyi*.

In the previous work (Zhang et al., 2019), we transferred *E. huxleyi* cells stepwise from 80 μmol photons m^{-2} s^{-1} to 120 μmol photons m^{-2} s^{-1}, then to 200 μmol photons m^{-2} s^{-1}, to 320 μmol photons m^{-2} s^{-1} and to 480 μmol photons m^{-2} s^{-1} at both LC and HC levels under HNHP, LNHP or HNLP conditions, respectively. In this study, we transferred the same strain from LL to HL under HNHP condition, and then from HNHP to LNHP or HNLP, and from HNLP to LNLP under HL conditions under 4 "baseline" CO_2 and temperature treatments, in an effort to elucidate interactive and combined effects of temperature, CO_2, DIN and DIP (Table S2), in contrast the previous work carried out under constant temperature (Zhang et al., 2019).

2.2 Nutrient concentrations and carbonate chemistry measurements

In the first and last days of the incubations, 20 mL samples for determination of inorganic nitrogen and phosphate concentrations were taken at the same time using a filtered syringe (0.22 μm pore size, Haining) and measured by using a scanning spectrophotometer (Du 800, Beckman Coulter) according to Hansen and Koroleff (1999). The nitrate was reduced to nitrite by zinc cadmium reduction and then total nitrite concentration was measured. In parallel, 25 mL samples were taken for determination of total alkalinity (TA) after being filtered (0.22 μm pore size, Syringe Filter) under moderate pressure using a pump (GM-0.5A, JINTENG) and stored in the dark at 4 °C for less than 7 d. TA was measured at 20 °C by potentiometric titration (AS-ALK1+, Apollo SciTech) according to Dickson et al. (2003). Samples for pH_T (total scale) determinations were syringe-filtered (0.22 μm pore size), and the bottles were filled from bottom to top with overflow and closed immediately without headspace. The pH_T was immediately measured at 20 °C by using a pH meter (Benchtop pH, Orion 8102BN) which was calibrated with buffers (Tris•HCl, Hanna) at pH 4.01, 7.00 and 10.00. Carbonate chemistry parameters were calculated from TA, pH_T, phosphate (at 1.5 μmol L^{-1} or 0.5 μmol L^{-1}), temperature (at 16 °C or 20 °C), and salinity using the CO_2 system calculation in MS Excel software (Pierrot et al., 2006). K_1 and K_2, the first and second carbonic acid constants, were taken from Roy et al. (1993).

2.3 Cell concentration measurements

In the last day of the incubation, ~25 mL samples (8 samples) were taken at the same time (about 1:00 p.m.). Cell concentration and cell diameter (D) were measured using

a Z2 Coulter Particle Count and Size Analyzer (Beckman Coulter). The diameter of detected particles was set to be 3 to 7 μm in the instrument, which excludes detached coccoliths (Müller et al., 2012). Cell concentration was also measured by microscopy (ZEISS), and variation in measured cell concentration between two methods was ± 7.9% (Zhang et al., 2019). Average growth rate (μ) was calculated for each replicate according to the equation: $\mu = (\ln N_1 - \ln N_0) / d$, where N_0 was 150 cells mL^{-1} and N_1 was the cell concentration in the last day of the incubation, d was the growth period in days. *E. huxleyi* cells were spherical and its cell volume with coccoliths was calculated according to the equation: $V = 3.14 \times (4/3) \times (D/2)^3$.

2.4 Total particulate (TPC) and particulate organic (POC) carbon measurements

100 mL samples for determination of TPC and POC quotas were filtered onto GF/F filters (pre-combusted at 450 °C for 6 h) at the same time in each treatment. TPC and POC samples were stored in the dark at –20 °C. For POC measurements, samples were fumed with HCl for 12 h to remove inorganic carbon, and samples for TPC measurements were not treated with HCl. All samples were dried at 60 °C for 12 h, and analyzed using a Thermo Scientific FLASH 2000 CHNS/O elemental analyzer (Thermo Fisher, Waltham, MA). Particulate inorganic carbon (PIC) quota was calculated as the difference between TPC quota and POC quota. POC and PIC production rates were calculated by multiplying cellular contents with μ (d^{-1}), respectively. Variations in measured carbon content between the four replicates were calculated to be 1–24% in this study.

2.5 Data analysis

299 Firstly, we examined the interactions of temperature, pCO_2 and light under nutrient-
300 replete (HNHP) conditions. Here, the effects of temperature, pCO_2, light intensity and
301 their interaction on growth rate, POC and PIC quotas were tested using a three-way
302 analysis of variance (ANOVA). Secondly, we examined the effects of nutrient
303 limitation in the different pCO_2 and temperature environments under the high light
304 intensity (HL). Here, the effects of temperature, pCO_2, dissolved inorganic nitrogen
305 (DIN), dissolved inorganic phosphate (DIP) and their interaction on growth rate, POC
306 and PIC quotas were tested using a four-way ANOVA. Finally, a one-way ANOVA
307 was used to test the differences in growth rate, POC and PIC quotas between present
308 (defined as low levels of pCO_2, temperature and light along with high levels of DIN
309 and DIP (LC LT LL HN HP)) and future ocean (defined as higher levels of pCO_2,
310 temperature, and light along with low levels of DIN and DIP (HC HT HL LN LP))
311 scenarios. A Tukey post hoc test was performed to identify the differences between
312 two temperatures, two pCO_2 levels, two DIN or two DIP treatments. Normality of
313 residuals was conducted with a Shapiro-Wilk's test, and a Levene test was conducted
314 graphically to test for homogeneity of variances. A generalized least squares (GLS)
315 model was used to stabilize heterogeneity if variances were non-homogeneous. All
316 statistical calculations were performed using *R* (R version 3.5.0).

317 In order to quantify the individual effect of nitrate concentration or phosphate
318 concentration on the physiological and biochemical parameters, we calculated the
319 change ratio (R) of physiological rates according to the equation: $R = | M_{\text{LNHP or HNLP}}$
320 $- M_{\text{HNHP}} | / M_{\text{HNHP}}$, where $M_{\text{LNHP or HNLP or HNHP}}$ respresents measured trait values in
321 LNHP or HNLP or HNHP conditions, and the '|' denotes the absolute value
322 (Schaum et al., 2013). We then calculated the expected growth rate, POC quota and
323 PIC quota in LNLP conditions based on the measured trait values in HNHP

conditions and the change ratios in LNHP and HNLP conditions according to a linear model: $E_{LNLP} = (1 - R_{LNHP} - R_{HNLP}) \times M_{HNHP}$ for growth rate and POC quota; $E_{LNLP} = (1+R_{LNHP}+R_{HNLP}) \times M_{HNHP}$ for PIC quota (Brennan and Collins, 2015). We tested the significant differences between the expected trait values (E_{LNLP}) and the measured trait values (M_{LNLP}) in LNLP conditions by a one-way ANOVA (Fig. S3). We also calculated the extent of synergy between LNHP and HNLP on growth rate, POC quota and PIC quota according to equation: $S = | E_{LNLP} - M_{HNHP} | / M_{HNHP}$. Please see the discussion section for more information.

3 Results

3.1 Carbonate chemistry parameters and nutrient concentrations

During the incubations, pH_T values increased due to organismal activity by, on average, 0.03 ± 0.01 in LCLT, by 0.01 ± 0.01 in HCLT, by 0.02 ± 0.01 in LCHT and by 0.02 ± 0.01 in HCHT conditions (Fig. 1f–j; Table 1). Correspondingly, seawater pCO_2 concentrations decreased by 8.8% ± 1.1% in LCLT, by 6.1% ± 4.4% in HCLT, by 6.6% ± 1.7% in LCHT, and by 5.4% ± 3.6% in HCHT conditions, respectively (Fig. 1k–o; Table 1).

During the incubations, dissolved inorganic nitrogen (DIN) concentrations decreased by 28.7% ± 6.7% in HNHP and LL (Fig. 1p), by 26.8% ± 5.9% in HNHP and HL (Fig. 1q), by 71.1% ± 3.3% in LNHP (Fig. 1r), by 32.9% ± 5.6% in HNLP (Fig. 1s), and by 69.8% ± 3.2% in LNLP conditions (Fig. 1t; Table 2). Dissolved inorganic phosphate (DIP) concentrations decreased by 62.2% ± 16.5% in HNHP and LL (Fig. 1u), by 71.3% ± 6.7% in HNHP and HL (Fig. 1v), by 61.0% ± 5.2% in LNHP (Fig. 1w), by 83.8% ± 5.4% in HNLP (Fig. 1x), and by 86.3% ± 1.4% in LNLP conditions (Fig. 1y; Table 2).

Overall, while organismal activity affected nutrient levels during growth cycles as expected, the high and low nutrient treatments remained different at all times (Table 2). Organismal activity had minimal effects on carbonate chemistry (see Fig. 1).

3.2 Population growth rate

Growth rate was significantly lower under the future scenario (HCHT HL LNLP: high levels of pCO_2, temperature and light as well as low levels of nutrients) than under the present scenario (LCLT LL HNHP: low levels of pCO_2, temperature and light alongside high levels of nutrients) (one-way ANOVA, $F = 52.6$, $p < 0.01$) (Figs. 2a and 3a,d; Table 2). The effect of increasing pCO_2 on growth rate is negative at low light or low nutrients levels, which can be seen by comparing population growth in all of the HC regimes with their paired LC regimes (Figs. 3a,b,e and S4). The extent of reduction in population growth rate depends on which other stressors are present. Compared to present atmospheric pCO_2 levels (LC, Fig. 3a), growth rates under ocean acidification (HC, Fig. 3b) decreased by an average of 17.4% ± 1.3% in HNHP and LL, and by an average of 4.4% ± 1.1% in HNHP and HL conditions (three-way ANOVA, both $p < 0.01$; Tukey post hoc test, both $p < 0.01$) (Fig. 3e; Tables 2 and 3), by 7.6% ± 2.6% in LNHP, by 21.4% ± 0.2% in HNLP, and by 32.1% ± 0.5% in LNLP conditions under the HL, respectively (four-way ANOVA, all $p < 0.01$; Tukey post hoc test, all $p < 0.01$) (Fig. 3a,b,e; Tables 2 and 4).

Across all HT/LT (high/low temperature) regime pairs, population growth rate is faster in the HT regimes, indicating that increasing temperature from 16 to 20 °C increases population growth rate in *E. huxleyi* (Figs. 3a,c,f and S4). Compared to the low temperature (LT, Fig. 3a), growth rates at the high temperature (HT, Fig. 3c) increased by 7.7% ± 0.7% in HNHP and LL, and by 34.0% ± 0.4% in HNHP and HL

conditions (three-way ANOVA, both $p < 0.01$; Tukey post hoc test, both $p < 0.01$) (Fig. 3a,c,f; Tables 2 and 3), by 42.4% ± 0.4% in LNHP, by 33.5% ± 0.5% in HNLP, and by 40.4% ± 3.1% in LNLP conditions under HL (four-way ANOVA, all $p < 0.01$; Tukey post hoc test, all $p < 0.01$) (Fig. 3a,c,f; Tables 2 and 4). Compared to low pCO_2 and low temperature (LCLT, Fig. 3a), growth rates in high pCO_2 and high temperature environments (HCHT, Fig. 3d) increased by 3.9% ± 0.9% in HNHP and LL, and by 31.1% ± 0.1% in HNHP and HL conditions (three-way ANOVA, both $p < 0.01$; Tukey post hoc test, both $p < 0.01$) (Fig. 3a,d,g; Tables 2 and 3), by 38.6% ± 0.1% in LNHP and by 17.1% ± 1.7% in HNLP, whereas growth rate decreased by 12.1% ± 2.2% in LNLP conditions under HL, respectively (four-way ANOVA, all $p < 0.01$; Tukey post hoc test, all $p < 0.01$) (Fig. 3a,d,g; Tables 2 and 4). These results show that high pCO_2, low nitrate and low phosphate concentrations collectively reduced the population growth rate in *E. huxleyi*, though elevated temperature could counteract this response.

The effects of reduced availability of nutrients on growth are nutrient-specific (Fig. 3). Compared to HNHP and HL, growth rates in LNHP decreased by 3.0–12.1% (all $p < 0.05$ at LCLT, HCLT, LCHT and HCHT conditions) (Fig. 3h; Tables 2 and 4). In contrast, HNLP did not significantly affect growth in LC conditions ($p > 0.1$ in LCLT and LCHT conditions) (Fig. 3a,c,i), but did lower population growth rate by 11.3–19.2% in HC conditions (both $p < 0.01$ at HCLT and HCHT conditions) (Fig. 3b,d,i). Unsurprisingly, when both nitrate and phosphate levels were reduced, growth rates always decreased by larger extent compared to environments where they were reduced individually (Fig. 3h,i,j). Compared to growth rates in HNHP and HL, growth rates in LNLP were 4.8–10.2% lower in LC environments, and 34.7–40.3% lower in HC environments (Tukey post hoc test, all $p < 0.01$ at LCLT, HCLT, LCHT and

HCHT conditions) (Fig. 3a–d,j; Tables 2 and 4). In summary, nitrate and phosphate limitation exacerbated the impacts of OA and warming on population growth rate.

3.3 POC quota

Cellular POC quotas were two-fold larger under the future scenario (HCHT HL LNLP) than under the current scenario (LCLT LL HNHP) (one-way ANOVA, $F = 96.1$, $p < 0.01$, Figs. 2b and 4a,d). The effect of increasing pCO_2 on POC quota is positive, regardless of other drivers present, which can be seen by comparing POC quotas in all of the HC regimes with their paired LC regimes (Figs. 4a,b,e and S4), though the extent of increase in POC quota depends on which other stressors are present. Compared to current atmospheric pCO_2 level (LC, Fig. 4a), POC quotas under ocean acidification (Fig. 4b) increased by 40.3% ± 10.1% in HNHP and LL (Tukey post hoc test, $p < 0.01$), by 13.8% ± 10.1% in HNHP and HL ($p = 0.47$), by 33.2% ± 11.1% at LNHP, by 109.4% ± 14.0% in HNLP and by 87.3% ± 10.8% in LNLP conditions under HL, respectively (four-way ANOVA, all $p < 0.01$; Tukey post hoc test, all $p < 0.01$) (Fig. 4a,b,e; Tables 2 and 4).

The effect of elevated temperature on POC quota can be seen by comparing POC quota in all of the HT regimes with their paired LT regimes (Figs. 4a,c,f and S4). Across all HT/LT regime pairs, POC quotas did not show significant differences between the HT and LT regimes under HNHP and LL, HNHP and HL, LNHP, HNLP and LNLP conditions under HL, respectively (Tukey post hoc test, all $p > 0.1$) (Fig. 4a,c,f). This demonstrated that increasing temperature within the test range had no significant effect on POC quota. The combined effects of increasing pCO_2 and temperature on POC quotas were nutrient dependent. Compared to low pCO_2 and low temperature (LCLT, Fig. 4a), POC quotas at high pCO_2 and high temperature (HCHT,

Fig. 4d) did not show significant differences in HNHP and LL (p = 0.79), in HNHP and HL (p = 0.99), and in LNHP and HL (p = 0.99), but increased by 52.2% ± 20.6% in HNLP and by 45.6% ± 14.8% in LNLP conditions under HL (Tukey post hoc test, both $p < 0.01$) (Fig. 4a,d,g; Tables 2 and 4). These data showed that high pCO_2 and low phosphate concentrations enhanced POC quotas of *E. huxleyi*, and that their combined effects were partly reduced by rising temperature.

The effects of nutrient reduction on POC quota are nutrient specific (Fig. 4). Compared to HNHP and HL, POC quotas in LNHP did not show a significant difference (all $p > 0.1$ at LCLT, HCLT, LCHT and HCHT) (Fig. 4a–d,h; Tables 2 and 4). At LC, POC quotas did not significantly differ between HNHP, HNLP and LNLP conditions (Tukey post hoc test, all $p > 0.1$) (Fig. 4a,c,i,j). In contrast, in HC, they were 43.3–78.2% larger in HNLP or LNLP than in HNHP (all $p < 0.01$) (Fig. 4b,d,i,j; Table 2).

3.4 PIC quota

Cellular PIC quotas were significantly larger in the future scenario with high levels of pCO_2, temperature and light along with low nutrients concentrations, than PIC quotas in the present scenario with low levels of pCO_2, temperature and light along with relatively high nutrients concentrations (one-way ANOVA, F = 63.6, $p < 0.01$) (Figs. 2c and 5a,d). However, the opposite results were found under the elevated CO_2 treatment alone. The effect of increasing pCO_2 on PIC quota is negative, regardless of presence of other drivers. By comparing PIC quota in all of the HC regimes with their paired LC regimes (Figs. 5a,b,e and S4), the effects of elevated pCO_2 level are clear, though the extent of reduction in PIC quota depends on which other stressors are present. Compared to present atmospheric pCO_2 levels (LC, Fig. 5a), PIC quotas

under ocean acidification (Fig. 5b) are reduced by 31.8% ± 17.1% in HNHP and LL, by 34.3% ± 10.0% in HNHP and HL, by 25.0% ± 3.8% in LNHP, by 22.8% ± 6.3% in HNLP and by 44.6% ± 0.9% in LNLP conditions under HL, respectively (Tukey post hoc test, all $p < 0.05$) (Fig. 5a,b,e; Tables 2–4). The extent of reduction in PIC quota is larger under LNLP conditions.

The effects of rising temperature on PIC quota were nutrient dependent, and can be seen by comparing PIC quotas in the HT regimes with those in their paired LT regimes (Figs. 5a,c,f and S4). Compared to low temperature (LT, Fig. 5a), PIC quotas at high temperature (HT, Fig. 5c) did not show significant differences in HNHP and LL, in HNHP and HL, in LNHP, and in HNLP conditions (Tukey post hoc test, all $p > 0.05$), whereas they decreased by 27.9% ± 8.4% in LNLP conditions under HL (Tukey post hoc test, $p < 0.01$) (Fig. 5a,c,f; Tables 2–4). The combined effects of rising pCO_2 and temperature on PIC quota are negative, regardless of which other drivers are present (Fig. 5a,d,g). Compared to low pCO_2 and low temperature (LCLT, Fig. 5a), PIC quotas in high pCO_2 and high temperature (HCHT, Fig. 5d) declined by 11.1% ± 10.9% in HNHP and LL ($p = 0.96$), by 32.5% ± 2.4% in HNHP and HL ($p < 0.01$), by 42.2% ± 3.2% in LNHP ($p < 0.01$), by 10.2% ± 7.7% in HNLP ($p = 0.92$), and by 45.3% ± 5.9% in LNLP conditions under HL, respectively ($p < 0.01$) (Fig. 5a,d,g; Table 2).

Effects of both nitrate and phosphate reduction on PIC quota are positive, regardless of levels of pCO_2 and temperature for the range used here (Fig. 5h,i,j). Compared to HNHP and HL, PIC quotas were larger in LNHP (Tukey post hoc test, $p < 0.01$ in LCLT, HCLT and LCHT conditions; $p = 0.73$ at HCHT condition) (Fig. 5h), in HNLP, and in LNLP conditions, respectively (all $p < 0.01$ at LCLT, HCLT, LCHT and HCHT conditions) (Fig. 5a–d,i,j; Table 2). In addition, PIC quotas were larger in

LNLP than in HNLP conditions (Tukey post hoc test, $p < 0.01$ in LCLT and HCLT conditions; $p = 0.06$ in LCHT; $p = 0.21$ in HCHT conditions) (Fig. 5a–d,i,j). These data showed that low nitrate and phosphate concentrations act synergistically to increase PIC quotas, which was moderated under the high pCO_2.

3.5 PIC / POC value

The ratio of PIC to POC (PIC / POC value) was not significantly different between the future scenario (HCHT HL LNLP) and the current scenario (LCLT LL HNHP) (one-way ANOVA, $F = 0.3$, $p = 0.60$) (Figs. 2d and 6a,d). The PIC / POC value followed the same trend as for PIC quotas described above. The effect of increasing pCO_2 on PIC / POC value was negative, regardless of which other drivers were present (Figs. 6a,b,e and S4), but the extent of reduction in PIC / POC value depended on presence of other drivers. Compared to current atmospheric pCO_2 levels (LC, Fig. 6a), PIC / POC values under ocean acidification (HC, Fig. 6b) decreased by 50.7% ± 18.2% in HNHP and LL, by 41.8% ± 15.4% in HNHP and HL, by 43.9% ± 5.8% in LNHP, by 63.0% ± 4.2% in HNLP, and by 70.7% ± 2.0% in LNLP conditions under HL, respectively (Tukey post hoc test, all $p < 0.05$) (Fig. 6a,b,e; Table 2).

The effect of rising temperature on PIC / POC value was nutrient dependant (Figs. 6a,c,f and S4). Compared to low temperature (LT, Fig. 6a), PIC / POC values at high temperature (HT, Fig. 6c) did not show significant differences in HNHP and LL, in HNHP and HL, in LNHP, and in LNLP conditions (Tukey post hoc test, all $p > 0.1$), whereas they increased by 39.0% ± 8.9% in HNLP conditions (Tukey post hoc test, $p = 0.006$) (Fig. 6a,c,f; Table 2). The combined effects of elevated pCO_2 and temperature on PIC / POC values were negative (Fig. 6a,d,g). Relative to low pCO_2 and low temperature (LCLT, Fig. 6a), PIC / POC values at high pCO_2 and high

499 temperature (HCHT, Fig. 6d) did not show significant differences in HNHP and LL,
500 and in HNHP and HL conditions (Tukey post hoc test, both $p > 0.1$), but they
501 decreased by 39.9% ± 3.0% in LNHP, by 40.6% ± 5.8% in HNLP, and by 67.8% ±
502 3.1% in LNLP conditions under HL, respectively (Tukey post hoc test, all $p < 0.01$)
503 (Fig. 6a,d,g; Table 2).

504 Across all LNHP/HNHP (low/high nitrate) regime pairs, PIC / POC values were
505 higher in the LNHP regime (Fig. 6h), though the extent of increase in PIC / POC
506 values depended on pCO_2 or temperature levels. Compared to HNHP and HL, PIC /
507 POC values in LNHP were about 106.0% ± 13.0% larger (Tukey post hoc test, $p <$
508 0.05 in LCLT and LCHT conditions; $p > 0.05$ in HCLT and HCHT conditions) (Fig.
509 6a–d, h; Table 2). The effect of phosphate on PIC / POC value also depended on
510 pCO_2 levels (Fig. 6i). In LC, PIC / POC values were larger in HNLP than in HNHP (p
511 = 0.22 at LCLT; $p < 0.05$ at LCHT conditions), and in LNLP than in LP ($p < 0.01$ at
512 LCLT; $p = 0.09$ in LCHT conditions) (Fig. 6a,c). In HC conditions, PIC / POC values
513 did not show significant differences among HNHP, HNLP and LNLP conditions
514 (Tukey post hoc test, all $p > 0.05$ in HCLT and HCHT conditions) (Fig. 6b,d; Table 2).
515

516 **4 Discussion**

517 Understanding effects of multiple drivers is helpful for improving how
518 coccolithorphores are represented in models (Krumhardt et al., 2017). Responses of
519 growth, POC and PIC quotas to ocean acidification have been shown to be modulated
520 by temperature (Gafar and Schulz, 2018; Tong et al., 2019), light intensity or light
521 period (light : dark cycle) (Jin et al., 2017; Bretherton et al., 2019), DIN or DIP
522 concentrations (Müller et al., 2017), combinations of light intensity and nutrients
523 availability (Zhang et al., 2019) (Table 5). Following up our previous study (Zhang et

al., 2019), we added temperature as a key driver of 5 drivers (Table S2), and explored how temperature changes would modulate the combined effects of CO_2, light, DIN and DIP that we previously reported. Our data showed that a future ocean climate change cluster (increasing CO_2, temperature, and light levels along with decreasing DIN and DIP levels) can lower growth rate with increased POC and PIC quota per cell (Fig. 2) as a result of plastic responses to the drivers. In contrast, observations of coccolithophore Chl *a* increased from 1990 to 2014 in the North Atlantic, and rising CO_2 and temperature has been aassociated with accelerated growth of coccolithophores since 1965 in the North Atlantic (Rivero-Calle et al., 2015; Krumhardt et al., 2016). Our results from laboratory experiments with multiple drivers experiment instead predicted a different trend with progressive ocean climate changes. We have to admit that results from laboratory experiments can hardly extrapolate to natural conditions. Nevertheless, our data provide mechanistic understanding of the combined effects of ocean climate change drivers, which can be useful in analyzing field observations.

It should also be noted that regional responses to ocean global changes could differ due to chemical and physical environmental differences and species and strain variability among different oceans or regions (Blanco-Ameijeiras et al., 2016; Gao et al., 2019), and that this could also explain discrepancies between experiments and observations. Different *E. huxleyi* strains displayed optimal responses to a broad range of temperature or CO_2 level, and *E. huxleyi* strains isolated from different regions showed local adaptation to temperature or CO_2 level (Zhang et al., 2014; 2018). Strain-specific responses of growth, POC and PIC production rates in *E. huxleyi* isolated from different regions to changing seawater carbonate chemistry have also been documented (Langer et al., 2009). It has been suggested that inter-strain genetic

549 variability has greater potential to induce larger phenotypic differences than the
550 phenotypic plasticity of a single strain cultured under a broad range of variable
551 environmental conditions (Blanco-Ameijeiras et al., 2016). On the other hand, the
552 genetic adaptation to culture experimental conditions over time may no longer
553 accurately represent the cells in the sea, as reflected in a diatom (Guan and Gao, 2008).
554 Phytoplankton species that had been maintained under laboratory conditions might
555 have lost original traits and display different responses to environmental changes
556 (Lakeman et al., 2009). The strain used in this study has been kept in the laboratory
557 for about 30 years, and the data obtained in this work can hardly reflect relation to its
558 biogeographic origin.

559 The decreased availability of nitrate or phosphate individually reduced growth rate
560 and increased PIC quota, respectively, in this experiment. Furthermore, under LNLP
561 and high pCO_2 levels, measured growth rates were significantly lower than the
562 expected values estimated on the basis of the values in LNHP and HNLP conditions
563 (Fig. S3a). This indicates synergistic negative effects of LN and LP on growth rate, an
564 evidence that colimitation of N and P is more severe than that by N or P alone. Here,
565 the extent of synergy between LN and LP on growth rate was calculated to be
566 8.6%±2.8% at low temperature and to be 40.6%±3.8% at high temperature (Fig. S3a),
567 suggesting modulating effect of temperature on response of growth rate to nutrient
568 limitations (Thomas et al., 2017). Similarly, at LNLP and low pCO_2 level, the
569 measured PIC quota was significantly larger than the expected value (Fig. S3c),
570 indicating synergistic positive effects of LN and LP on PIC quota, with the extent of
571 synergy being 31.4%±3.9% at low temperature. LN and LP did not synergistically act
572 to reduce POC quota.

While there were always interactions among stressors, increased temperature itself sped up population growth to a relatively consistent value at high light, regardless of nutrient limitation, with statistically significant but small differences over the different nutrient regimes (Fig. 3f). Rising pCO_2 level not only decreased the absolute values of growth rate, but also reduced the positive effect of high temperature on growth. In addition, elevated pCO_2 also altered patterns of growth responses to changes in light and nutrient levels (Fig. 3e–g). In ocean acidification condition, the negative effect of low pH on growth rate of the same *E. huxeyi* strain PML B92/11 was larger than the positive effect of high CO_2 concentration (Bach et al., 2011). Our data further showed that low-pH inhibited growth to lesser extent under the high light than under low light (Fig. 3e; Table 2). One possible explanation for this could be that photosynthesis under the high light regime could generate more energy-conserving compounds (Fernández et al., 1996). This results in faster pCO_2 removal and counteracts the negative effects of low pH. This interaction between low pH and high light was also observed when *E. huxleyi* strains PML B92/11 and CCMP 2090 were grown under incident sunlight (Jin et al., 2017).

Increases in temperature reduced PIC quotas under some conditions (high light (HL), HL-LNHP and HL-LNLP) (Fig. 5f), suggesting that the ratio of N:P is important in modulating calcification under warming. One striking result is the consistent negative effect of high pCO_2 on growth and PIC quota, regardless of other stressors. While pCO_2 levels affected the absolute PIC values, the combination of high pCO_2 and warming did not affect the responses to light and nutrients once the direct reduction in PIC quota due to increased pCO_2 was taken into account (Fig. 5g). It has been documented that PIC quotas of *E. huxleyi* strain PML B92/11 reduced at high pCO_2 due to suppressed calcification (Riebesell and Tortell, 2011). This

knowledge has been based on experiments under nutrient-replete or constant conditions without consideration of multiple drivers. In this work, PIC quota of *E. huxleyi* under OA were raised with increased light intensity and decreased availability of nutrients (Figs. 2 and 5). These results are consistent with other studies (Perrin et al., 2016; Jin et al., 2017), which reported that nutrient limitations enhanced calcification, and high light intensity could make cells to remove H^+ faster and then reduce the negative effect of low pH on calcification of *E. huxleyi* (Jin et al., 2017). Our data also indicate that effects of ocean climate change on calcification of *E. huxleyi* are more complex than previously thought (Meyer and Riebesell, 2015). It is worth noting that the observed higher POC and PIC quotas under future ocean climate change scenario could be attributed to cell cycle arrest of a portion of the community (Vaulot et al., 1987). Decreased availabilities of nitrate and phosphate can extend the G1 phase where photosynthetic carbon fixation and calcification occurred, and lead to lower dark respiration which reduces carbon consumption (Vaulot et al., 1987; Müller et al., 2008; Gao et al., 2018).

Synthesis of RNA is a large biochemical sink for phosphate in *E. huxleyi* and other primary producers (Dyhrman, 2016). In this study, RNA content per cell was verified by a SYBR Green method (Berdalet et al., 2005). Compared to HNHP conditions, HNLP-grown cells had only 7.8% of total RNA (Fig. S11). This indicates that decreased availability of phosphate strongly decreased RNA synthesis, which would consequently extend the interphase of the cell cycle where calcification occurs (Müller et al., 2008). This could explain why PIC quotas were enhanced by decreased phosphate availability (Fig. 5). Similarly, decreased availability of nitrate decreased protein (or PON) synthesis (Fig. S10), which can also block cells in the interphase of the cell cycle, and increase the time available for calcification in *E. huxleyi* (Vaulot et

623 al., 1987). Consistently with this, lower rates of assimilation or organic matter
624 production in *E. huxleyi* in LNHP than in HNHP treatments are consistent with more
625 energy being reallocated to use for calcification (Nimer and Merrett, 1993; Xu and
626 Gao, 2012).

627 Low phosphate concentrations can induce high affinity phosphate uptake in *E.*
628 *huxleyi* (Riegman et al., 2000; Dyhrman and Palenik, 2003; McKew et al., 2015). This
629 mechanism enables *E. huxleyi* to take up phosphate efficiently at low pCO_2
630 concentrations, so that no significant difference in growth rate was observed between
631 HNLP and HNHP treatments (Fig. 3a,c). However, at high pCO_2, low phosphate
632 concentration (HNLP) lowered growth of *E. huxleyi* relative to HNHP (Fig. 3a–d;
633 Table 2). While the affinity of *E. huxleyi* for phosphate under different pCO_2 levels
634 has not been studied, the extra energetic cost of coping with stress from high pCO_2
635 could limit the energy available for the active uptake of phosphate. In addition, the
636 activity of alkaline phosphatase, which might work to reuse released organic P,
637 decreases at low pH (Rouco et al., 2013). Finally, the enlarged cell volume in HC and
638 HNLP (or LNLP) conditions may further reduce nutrient uptake by cells due to
639 reduced surface to volume ratios, and lower cell division rates (Fig. S5) (Finkel, 2001).
640 While substantial evolutionary responses to multiple drivers may help further, our
641 results imply that decreased phosphate availability along with progressive ocean
642 acidification and warming in surface ocean may reduce the competitive capability of
643 *E. huxleyi* in oligotrophic waters. Meanwhile, HNLP also affected expressions of
644 genes related to nitrogen metabolism due to the tight stoichiometric coupling of
645 nitrogen and phosphate metabolism (Rokitta et al., 2016). Decreased availability of
646 nitrate further limited nitrogen metabolism of *E. huxleyi* (Rokitta et al., 2014), which
647 lowered the overall biosynthetic activity and reduced cellular PON quotas (Fig. S10).

These explain the synergistic inhibitions of low-pH, low-phosphate and low-nitrate on growth of *E. huxleyi* (Fig. 3).

POC quotas and the cell-volume normalized POC quotas were larger at high pCO_2 than at low pCO_2 under all treatments (Figs. 4; S6; Table 2), which could be a combined outcome of increased photosynthetic carbon fixation (Zondervan et al., 2002; Hoppe et al., 2011; Tong et al., 2019) and reduced cell division (present work), leading to pronounced increase of POC quotas in the cells grown under low phosphate (HNLP) and high pCO_2 (Fig. 4). At HNLP and high pCO_2 levels, photosynthetic carbon fixation proceeds whereas cell division rate decreases (Figs. 3 and 4), so reallocation of newly produced particulate organic carbon (POC) could be slowed down (Vaulot et al., 1987). In this case, over-synthesis of cellular organic carbon might be released as dissolved organic carbon (DOC), which can coagulate to transparent exopolymer particles (TEP) and attach to cells (Biermann and Engel, 2010; Engel et al., 2015). When cells were filtered on GF/F filters, any TEP would not have be separated from the cells and would have contributed to the measured POC quota in this study.

Large PIC quotas of coccolithophores may facilitate accumulation of calcium carbonate in the deep ocean and increase the contribution of $CaCO_3$ produced by coccolithophores to calcareous ooze in the pelagic ocean (Hay, 2004). Due to $CaCO_3$ being more dense than organic carbon, larger PIC quotas may facilitate effective transport of POC to deep oceans, leading to vertical DIC or CO_2 gradients of seawater (Milliman, 1993; Ziveri et al., 2007). While the effects of global ocean climate changes on physiological processes of phytoplankton can be complex, our results promote our understanding on how a cosmopolitan coccolithophore responds to future ocean environmental changes through plastic trait change.

673

674

675

676 *Data availability.* The data are available upon request to the corresponding author
677 (Kunshan Gao).

678

679

680

681 *Author contributions*. YZ, KG designed the experiment. YZ performed this
682 experiment. All authors analysed the data, wrote and improved the manuscript.

683

684

685

686 *Competing interests*. The authors declare that they have no conflict of interest.

687

688

689

690 *Acknowledgements*. This study was supported by National Natural Science
691 Foundation of China (41720104005, 41806129, 41721005), and Joint Project of
692 National Natural Science Foundation of China and Shandong province (No.
693 U1606404).

694

695

696

697

References

Bach, L. T., Riebesell, U., and Schulz, K. G.: Distinguishing between the effects of ocean acidification and ocean carbonation in the coccolithophore *Emiliania huxleyi*, Limnol. Oceanogr., 56, 2040–2050, doi: 10.4319/lo.2011.56.6.2040, 2011.

Barton, A. D., Irwin, A. J., Finkel, Z. V., and Stock, C. A.: Anthropogenic climate change drives shift and shuffle in North Atlantic phytoplankton communities, Proc. Nat. Aca. Sci. USA, 113, 2964–2969, doi:10.1073/pnas.1519080113, 2016.

Berdalet, E., Roldán, C., Olivar, M. P., and Lysnes, K.: Quantifying RNA and DNA in planktonic organisms with SYBR Green II and nucleases. Part A. Optimisation of the assay, Sci. Mar., 69, 1–16, doi: 10.3989/scimar.2005.69n11, 2005.

Biermann, A., and Engel, A.: Effect of CO_2 on the properties and sinking velocity of aggregates of the coccolithophore *Emiliania huxleyi*, Biogeosciences, 7, 1017–1029, doi :10.5194/bg-7-1017-2010, 2010.

Blanco-Ameijeiras, S., Lebrato, M., Stoll, H. M., Iglesias-Rodriguez, D., Müller, M. N., Méndez-Vicente, A., and Oschlies, A.: Phenotypic variability in the coccolithophore *Emiliania huxleyi*, Plos ONE, 11, e0157697, doi: 10.1371/journal.pone.0157697, 2016.

Borchard, C., Borges, A. V., Händel, N., and Engel, A.: Biogeochemical response of *Emiliania huxleyi* (PML B92/11) to elevated CO_2 and temperature under phosphorus limitation: A chemostat study, J. Exp. Mar. Biol. Ecol., 410, 61–71, doi: 10.1016/j.jembe.2011.10.004, 2011.

Boyd, P. W., Collins, S., Dupont, S., Fabricius, K., Gattuso, J. P., Havenhand, J., Hutchins, D. A., Riebesell, U., Rintoul, M. S., Vichi, M., Biswas, H., Ciotti, A.,

Gao, K., Gehlen, M., Hurd, C. L., Kurihara, H., McGraw, C. M., Navarro, J. M., Nilsson, G. E., Passow, U., and Pörtner, H. O.: Experimental strategies to assess the biological ramifications of multiple drivers of global ocean change—A review, Global Change Biol., 24, 2239–2261, doi: 10.1111/gcb.14102, 2018.

Boyd, P. W., Dillingham, P. W., McGraw, C. M., Armstrong, E. A., Cornwall, C. E., Feng, Y., Hurd, C. L., Gault-Ringold, M., Roleda, M. Y., Timmins-Schiffman, E., and Nunn, B. L.: Physiological responses of a Southern Ocean diatom to complex future ocean conditions, Nat. Clim. Change, 6, 207–213, doi: 10.1038/NCLIMATE2811, 2016.

Boyd, P. W., Lennartz, S. T., Glover, D. M., and Doney, S. C.: Biological ramifications of climate-change-mediated oceanic multi-stressors, Nat. Clim. Change, 5, 71–79, doi: 10.1038/nclimate2441, 2015.

Boyd, P. W., Strzepek, R., Fu, F., and Hutchins, D. A.: Environmental control of open-ocean phytoplankton groups: Now and in the future, Limnol. Oceanogr., 55, 1353–1376, doi: 10.4319/lo.2010.55.3.1353, 2010.

Brennan, G., and Collins, S.: Growth responses of a green alga to multiple environmental drivers, Nat. Clim. Change, 5, 892–897, doi: 10.1038/nclimate2682, 2015.

Brennan, G., Colegrave, N., and Collins, S.: Evolutionary consequences of multidriver environmental change in an aquatic primary producer, Proc. Nat. Aca. Sci. USA, 114, 9930–9935, doi: 10.1073/pnas.1703375114, 2017.

Bretherton, L., Poulton, A. J., Lawson, T., Rukminasari, N., Balestreri, C., Schroeder, D., Mark Moore, C., and Suggett, D. J.: Day length as a key factor moderating the response of coccolithophore growth to elevated pCO_2, Limnol. Oceanogr., 64, 1284–1296, doi: 10.1002/lno.11115, 2019.

748 De Bodt, C., Van Oostende, N., Harlay, J., Sabbe, K., and Chou, L.: Individual and
749 interacting effects of pCO_2 and temperature on *Emiliania huxleyi* calcification:
750 study of the calcite production, the coccolith morphology and the coccosphere
751 size, Biogeosciences, 7, 1401–1412, doi: 10.5194/bg-7-1401-2010, 2010.
752 Dickson, A. G., Afghan, J. D., and Anderson, G. C.: Reference materials for oceanic
753 CO_2 analysis: a method for the certification of total alkalinity, Mar. Chem., 80,
754 185–197, doi: 10.1016/S0304-4203(02)00133-0, 2003.
755 Dyhrman, S. T., and Palenik, B.: Characterization of ectoenzyme activity and
756 phosphate-regulated proteins in the coccolithophorid *Emiliania huxleyi*, J.
757 Plankton Res., 25, 1215–1225, doi: 10.1093/plankt/fbg086, 2003.
758 Dyhrman, S. T.: Nutrients and their acquisition: phosphorus physiology in microalgae,
759 in: The physiology of microalgae, edited by: Borowitzka, M. A., Beardall, J. and
760 Raven, J. A., Springer, Heidelberg, 155–183, doi: 10.1007/978-3-319-24945-2,
761 2016.
762 Engel, A., Borchard, C., Loginova, A. N., Meyer, J., Hauss, H., and Kiko, R.: Effects
763 of varied nitrate and phosphate supply on polysaccharidic and proteinaceous gel
764 particles production during tropical phytoplankton bloom experiments,
765 Biogeosciences, 12, 5647–5665, doi: 10.5194/bg-12-5647-2015, 2015.
766 Feng, Y., Roleda, M. Y., Armstrong, E., Boyd, P. W., and Hurd., C. L.:
767 Environmental controls on the growth, photosynthetic and calcification rates of a
768 southern hemisphere strain of the coccolithophore *Emiliania huxleyi*, Limnol.
769 Oceanogr., 62, 519–540, doi: 10.1002/lno.10442, 2017.
770 Feng, Y., Warner, M. E., Zhang, Y., Sun, J., Fu, F., Rose, J. M., and Hutchins, D. A.:
771 Interactive effects of increased pCO_2, temperature and irradiance on the marine

772 coccolithophore *Emiliania huxleyi* (Prymnesiophyceae), Eur. J. Phycol., 43, 87–
773 98, doi: 10.1080/09670260701664674, 2008.
774 Fernández, E., Fritz, J. J., and Balch, W. M.: Chemical composition of the
775 coccolithophorid *Emiliania huxleyi* under light-limited steady state growth. J.
776 Exp. Mar. Biol. Ecol., 207, 149–160. doi: 10.1016/S0022-0981(96)02657-3,
777 1996.
778 Finkel, Z. V.: Light absorption and size scaling of light-limited metabolism in marine
779 diatoms, Limnol. Oceanogr., 46, 86–94, doi: 10.4319/lo.2001.46.1.0086, 2001.
780 Gafar, N. A., and Schulz, K. G.: A three-dimensional niche comparison of *Emiliania*
781 *huxelyi* and *Gephyrocapsa oceanica*: reconciling observations with projections,
782 Biogeosciences, 15, 3541–3560, doi: 10.5194/bg-15-3541-2018, 2018.
783 Gao, G., Xia, J., Yu, J., and Zeng, X.: Physiological response of a red tide alga
784 (*Skeletonema costatum*) to nitrate enrichment, with special reference to inorganic
785 carbon acquisition, Mar. Environ. Res., 133, 15–23, doi:
786 10.1016/j.marenvres.2017.11.003, 2018.
787 Gao, K., Beardall, J., Häder, D. P., Hall-Spencer, J. M., Gao, G., and Hutchins, D. A.:
788 Effects of ocean acidification on marine photosynthetic organisms under the
789 concurrent influences of warming, UV radiation, and deoxygenation, Front. Mar.
790 Sci., 6, 322, doi: 10.3389/fmars.2019.00322, 2019.
791 Gao, K., Ruan, Z., Villafañe, V. E., Gattuso, J., and Walter-Helbling, E.: Ocean
792 acidification exacerbates the effect of UV radiation on the calcifying
793 phytoplankton *Emiliania huxleyi*, Limnol. Oceanogr., 54, 1855–1862, doi:
794 10.4319/lo.2009.54.6.1855, 2009.
795 Guan, W., and Gao, K.: Light histories influence the impacts of solar ultraviolet
796 radiation on photosynthesis and growth in a marine diatom, *Skeletonema*

costatum, J. Photoch. Photobio. B., 91, 151–156, doi: 10.1016/j.jphotobiol.2008.03.004, 2008.

Hansen, H. P., and Koroleff, F.: Determination of nutrients, in: Methods of seawater analysis, edited by: Grasshoff, K., Kremling, K. and Ehrhardt, M., WILEY-VCH Publishers, ISBN: 3-527-29589-5, 1999.

Hay, W. W.: Carbonate fluxes and calcareous nannoplankton, in: Coccolithophores: from molecular biology to global impact, edited by: Thierstein, H. R. and Young, J. R., Springer, Berlin, 509–528, 2004.

Hoppe, C. J. M., Langer, G., and Rost, B.: *Emiliania huxleyi* shows identical responses to elevated pCO_2 in TA and DIC manipulations, J. Exp. Mar. Biol. Ecol., 406, 54–62, doi: 10.1016/j.jembe.2011.06.008, 2011.

Jin, P., Ding, J. C., Xing, T., Riebesell, U., and Gao, K. S.: High levels of solar radiation offset impacts of ocean acidification on calcifying and non-calcifying strains of *Emiliania huxleyi*, Mar. Ecol. Prog. Ser., 568, 47–58, doi: 10.3354/meps12042, 2017.

Kottmeier, D. M., Rokitta, S. D., and Rost, B.: Acidification, not carbonation, is the major regulator of carbon fluxes in the coccolithophore *Emiliania huxleyi*, New Phytol., 211, 126–137, doi: 10.1111/nph.13885, 2016.

Krumhardt, K. M., Lovenduski, N. S., Iglesias-Rodriguez, M. D., and Kleypas, J. A.: Coccolithophore growth and calcification in a changing ocean, Prog. Oceanogr., 171, 276–295, doi: 10.1016/j.pocean.2017.10.007, 2017.

Krumhardt, K. M., Lovenduski, N. S., Freeman, N. M., and Bates, N. R.: Apparent increase in coccolithophore abundance in the subtropical North Atlantic from 1990 to 2014, Biogeosciences, 13, 1163–1177, doi: 10.5194/bg-13-1163-2016, 2016.

822 Kwiatkowski, L., Aumont, O., and Bopp, L.: Consistent trophic amplification of
823 marine biomass declines under climate change, Glob. Change Biol., 25, 218–229,
824 doi: 10.1111/gcb.14468, 2019.
825 Lakeman, M. B., von Dassow, P., and Cattolico, R. A.: The strain concept in
826 phytoplankton ecology, Harmful Algae, 8, 746–758, doi:
827 10.1016/j.hal.2008.11.011, 2009.
828 Langer, G., Nehrke, G., Probert, I., Ly, J., and Ziveri, P.: Strain-specific responses of
829 *Emiliania huxleyi* to changing seawater carbonate chemistry, Biogeosciences, 6,
830 2637–2646, doi: 10.5194/bg-6-2637-2009.
831 Larsen, A., Flaten, G. A. F., Sandaa, R., Castberg, T., Thyrhaug, R., Erga, S. R.,
832 Jacquet, S., and Bratbak, G.: Spring phytoplankton bloom dynamics in
833 Norwegian coastal waters: Microbial community succession and diversity,
834 Limnol. Oceanogr., 49, 180–190, doi: 10.4319/lo.2004.49.1.0180, 2004.
835 Leonardos, N., and Geider, R. J.: Elevated atmospheric carbon dioxide increases
836 organic carbon fixation by *Emilinia huxleyi* (haptophyta), under nutrient-limited
837 high-light conditions, J. Phycol., 41, 1196–1203, doi: 10.1111/j.1529-
838 8817.2005.00152.x, 2005.
839 Li, W., Yang, Y., Li, Z., Xu, J., and Gao, K.: Effects of seawater acidification on the
840 growth rates of the diatom *Thalassiosira (Conticribra) weissflogii* under
841 different nutrient, light and UV radiation regimes, J. Appl. Phycol., 29, 133–142,
842 doi: 10.1007/s10811-016-0944-y, 2017.
843 Locarnini, R. A., Mishonov, A. V., Antonov, J. I., Boyer, T. P., and Garcia, H. E.:
844 World ocean atlas 2005, V. 1: Temperature, edited by: Levitus, S., NOAA Atlas
845 NESDIS 61. U. S. Government Printing Office, 123–134, 2006.

Matthiessen, B., Eggers, S. L., and Krug, S. A.: High nitrate to phosphorus regime attenuates negative effects of rising pCO_2 on total population carbon accumulation, Biogeosciences, 9, 1195– 1203, doi: 10.5194/bg-9-1195-2012, 2012.

McKew, B. A., Metodieva, G., Raines, C. A., Metodiev, M. V., and Geider, R. J.: Acclimation of *Emiliania huxleyi* (1516) to nutrient limitation involves precise modification of the proteome to scavenge alternative sources of N and P, Environ. Microbiol., 17, 1–13, doi: 10.1111/1462-2920.12957, 2015.

Meyer, J., and Riebesell, U.: Reviews and syntheses: response of coccolithophores to ocean acidification: a meta-analysis, Biogeosciences, 12, 1671–1682, doi: 10.5194/bg-12-1671-2015, 2015.

Milliman, J. D.: Production and accumulation of calcium carbonate in the ocean: budget of a nonsteady state, Global Biogeochem. Cy., 7, 927–957, doi: 10.1029/93GB02524, 1993.

Monteiro, F. M., Bach, L. T., Brownlee, C., Bown, P., Rickaby, R. E. M., Poulton, A. J., Tyrrell, T., Beaufort, L., Dutkiewicz, S., Gibbs, S., Gutowska, M. A., Lee, R., Riebesell, U., Young, J., and Ridgwell, A.: Why marine phytoplankton calcify, Sci. Adv., 2, 1–14, doi: 10.1126/sciadv.1501822, 2016.

Müller, M. N., Antia, A. N., and LaRoche, J.: Influence of cell cycle phase on calcification in the coccolithophore *Emiliania huxleyi*, Limnol. Oceanogr., 53, 506–512, doi: 10.4319/lo.2008.53.2.0506, 2008.

Müller, M. N., Beaufort, L., Bernard, O., Pedrotti, M. L., Talec, A., and Sciandra, A.: Influence of CO_2 and nitrogen limitation on the coccolith volume of *Emiliania huxleyi* (Haptophyta), Biogeosciences, 9, 4155–4167, doi: 10.5194/bg-9-4155-2012, 2012.

Müller, M. N., Trull, T. W., and Hallegraeff, G. M.: Independence of nutrient limitation and carbon dioxide impacts on the Southern Ocean coccolithophore *Emiliania huxleyi*, The ISME J., 11, 1777–1787, doi: 10.1038/ismej.2017.53, 2017.

Nimer, N. A., and Merrett, M. J.: Calcification rate in *Emiliania huxleyi* Lohmann in response to light, nitrate and availability of inorganic carbon, New Phytol., 123, 673–677, doi: 10.1111/j.1469-8137.1993.tb03776.x, 1993.

Omar, A. M., Olsen, A., Johannessen, T., Hoppema, M., Thomas, H., and Borges, A. V.: Spatiotemporal variations of fCO_2 in the North Sea, Ocean Sci., 6, 77–89, doi: 10.5194/osd-6-1655-2009, 2010.

Perrin, L., Probert, I., Langer, G., and Aloisi, G.: Growth of the coccolithophore *Emiliania huxleyi* in light- and nutrient-limited batch reactors: relevance for the BIOSOPE deep ecological niche of coccolithophores, Biogeosciences, 13, 5983–6001, doi: 10.5194/bg-13-5983-2016, 2016.

Pierrot, D., Lewis, E., and Wallace, D. W. R.: MS Excel program developed for CO_2 system calculations, ORNL/CDIAC-105, Carbon Dioxide Information Analysis Centre, Oak Ridge National Laboratory, U.S., Department of Energy, doi: 10.3334/CDIAC/otg.CO2SYS_XLS_CDIAC105a, 2006.

R version 3.5.0.: The R foundation for statistical computing platform: x86_64-w64-mingw32/x64, 2018.

Riebesell, U., and Gattuso, J. P.: Lessons learned from ocean acidification research, Nat. Clim. Change, 5, 12–14, doi: 10.1038/nclimate2456, 2015.

Riebesell, U., and Tortell, P. D.: Effects of ocean acidification on pelagic organisms and ecosystems, in: Ocean acidification, edited by: Gattuso, J. P. and Hansson, L., Oxford University Press, 99–121, 2011.

Riegman, R., Stolte, W., Noordeloos, A. A. M., and Slezak, D.: Nutrient uptake and alkaline phosphatase (EC 3:1:3:1) activity of *Emiliania huxleyi* (Prymnesiophyceae) during growth under N and P limitation in continuous cultures, J. Phycol., 36, 87–96, doi: 10.1046/j.1529-8817.2000.99023.x, 2000.

Rivero-Calle, S., Gnanadesikan, A., Del Castillo, C. E., Balch, W. M., and Guikema, S. D.: Multidecadal increase in North Atlantic coccolithophores and the potential role of rising CO_2, Science, 350, 1533–1537, doi: 10.1126/science.aaa8026, 2015.

Rokitta, S. D., von Dassow, P., Rost, B., and John, U.: *Emiliania huxleyi* endures N-limitation with an efficient metabolic budgeting and effective ATP synthesis, BMC Genomics, 15, 1051–1064, doi: 10.1186/1471-2164-15-1051, 2014.

Rokitta, S. D., von Dassow, P., Rost, B., and John, U.: P- and N-depletion trigger similar cellular responses to promote senescence in eukaryotic phytoplankton, Front. Mar. Sci., 3, 109, doi: 10.3389/fmars.2016.00109, 2016.

Rosas-Navarro, A., Langer, G., and Ziveri, P.: Temperature affects the morphology and calcification of *Emiliania huxleyi* strains, Biogeosciences, 13, 2913–2926, doi: 10.5194/bg-13-2913-2016, 2016.

Rost, B., and Riebesell, U.: Coccolithophores and the biological pump: responses to environmental changes, in: Coccolithophores : from molecular biology to global impact, edited by: Thierstein, H. R. and Young, J. R., Springer, Berlin, 99–125, 2004.

Rost, B., Zondervan, I., and Riebesell, U.: Light-dependent carbon isotope fractionation in the coccolithophorid *Emiliania huxleyi*, Limnol. Oceanogr., 47, 120–128, doi: 10.2307/3069125, 2002

Rouco, M., Branson, O., Lebrato, M., and Iglesias-Rodríguez, M.: The effect of nitrate and phosphate availability on *Emiliania huxleyi* (NZEH) physiology

under different CO_2 scenarios, Front. Microbiol., 4, 1–11, doi: 10.3389/fmicb.2013.00155, 2013.

Roy, R. N., Roy, L. N., Vogel, K. M., Porter-Moore, C., Pearson, T., Good, C. E., Millero, F. J., and Campbell, D. C.: Thermodynamics of the dissociation of boric acid in seawater at S 5 35 from 0 degrees C to 55 degrees C, Mar. Chem., 44, 243–248, doi: 10.1016/0304-4203(93)90206-4, 1993.

Schaum, E., Rost, B., Millar, A. J., and Collins, S.: Variation in plastic responses of a globally distributed picoplankton species to ocean acidification, Nat. Clim. Change, 3, 298–302, doi: 10.1038/NCLIMATE1774, 2013.

Sett, S., Bach, L. T., Schulz, K. S., Koch-Klavsen, S., Lebrato, M., and Riebesell, U.: Temperature modulates coccolithophorid sensitivity of growth, photosynthesis and calcification to increasing seawater pCO_2, PLoS One, 9(2), e88308, doi: 10.1371/journal.pone.0088308, 2014.

Sunda, W. G., Price, N. M., and Morel, F. M. M.: Trace metal ion buffers and their use in culture studies, in: Algal culturing techniques, edited by: Andersen, R. A., Elsevier Academic Press, 53–59, 2005.

Thomas, M. K., Aranguren-Gassis, M., Kremer, C. T., Gould, M. R., Anderson, K., Klausmeier, C. A., Litchman, E.: Temperature-nutrient interactions exacerbate sensitivity to warming in phytoplankton, Global Change Biol., 23, 3269–3280, doi: 10.1111/gcb.13641, 2017.

Tong, S., Hutchins, D., and Gao, K.: Physiological and biochemical responses of *Emiliania huxleyi* to ocean acidification and warming are modulated by UV radiation, Biogeosciences, 16, 561–572, doi: 10.5194/bg-16-561-2019, 2019.

Tong, S., Hutchins, D., Fu, F., and Gao, K.: Effects of varying growth irradiance and nitrogen sources on calcification and physiological performance of the

946 coccolithophore *Gephyrocapsa oceanica* grown under nitrogen limitation,
947 Limnol. Oceanogr., 61, 2234–2242, doi: 10.1002/lno.10371, 2016.
948 Vaulot, D., Olson, R. J., Merkel, S., and Chisholm, S. E.: Cell-cycle response to
949 nutrient starvation in two phytoplankton species, *Thalassiosira weissflogii* and
950 *Hymenomonas carterae*, Mar. Biol., 95, 625–630, doi: 10.1007/BF00393106,
951 1987.
952 Xu, J., Gao, K., Li, Y., and Hutchins, D. A.: Physiological and biochemical responses
953 of diatoms to projected ocean changes, Mar. Ecol. Prog. Ser., 515, 73–81, doi:
954 10.3354/meps11026, 2014b.
955 Xu, K., Fu, F., and Hutchins, D. A.: Comparative responses of two dominant
956 Antarctic phytoplankton taxa to interactions between ocean acidification,
957 warming, irradiance, and iron availability, Limnol. Oceanogr., 59, 1919–1931,
958 doi: 10.4319/lo.2014.59.6.1919, 2014a.
959 Xu, K., and Gao, K.: Reduced calcification decreases photoprotective capability in the
960 coccolithophorid *Emiliania huxleyi*, Plant Cell Physiol., 53, 1267–1274, doi:
961 10.1093/pcp/pcs066, 2012.
962 Xu, K., Gao, K., Villafañe, V. E., and Helbling, E. W.: Photosynthetic responses of
963 *Emiliania huxleyi* to UV radiation and elevated temperature: roles of calcified
964 coccoliths, Biogeosciences, 8, 1441–1452, doi: 10.5194/bg-8-1441-2011, 2011.
965 Zhang, Y., Bach, L. T., Lohbeck, K. T., Schulz K. G., Listmann, L., Klapper R., and
966 Riebesell, U.: Population-specific responses in physiological rates of *Emilinia*
967 *huxleyi* to a broad CO_2 range, Biogeosciences, 15, 3691–3701, doi: 10.5194/bg-
968 15-3691-2018, 2018.

Zhang, Y., Fu, F., Hutchins, D. A., and Gao. K.: Combined effects of CO_2 level, light intensity and nutrient availability on the coccolithophore *Emiliania huxleyi*, Hydrobiologia, 842, 127–141, doi: 10.1007/s10750-019-04031-0, 2019.

Zhang, Y., Klapper, R., Lohbeck, K. T., Bach, L. T., Schulz, K. G., Reusch, T. B. H., and Riebesell, U.: Between- and within-population variations in thermal reaction norms of the coccolithophore *Emiliania huxleyi*, Limnol. Oceanogr., 59, 1570–1580, doi: 10.4319/lo.2014.59.5.1570, 2014.

Ziveri, P., deBernardi, B., Baumann, K., Stoll, H. M., and Mortyn, P. G.: Sinking of coccolith carbonate and potential contribution to organic carbon ballasting in the deep ocean, Deep Sea Res., 54, 659–675, doi: 10.1016/j.dsr2.2007.01.006, 2007.

Zondervan, I., Rost, B., and Riebesell, U.: Effect of CO_2 concentration on the PIC/POC ratio in the coccolithophore *Emiliania huxleyi* grown under light-limiting conditions and different daylengths, J. Exp. Mar. Biol. Ecol., 272, 55–70, doi: 10.1016/s0022-0981(02)00037-0, 2002.

994 **Figure Legends**

995 **Figure 1.** Four "baseline" environments were used where pCO_2 and temperature
996 (temp) were combined in all pairwise combinations: low pCO_2 + low temp (LCLT,
997 △), high pCO_2 + low temp (HCLT, ✳), low pCO_2 + high temp (LCHT, □) and high
998 pCO_2 + high temp (HCHT, ○). Additional stressors were then added to each of the
999 four "baseline" environments. In step 1, low light (LL) was supplied. In step 2, high
1000 light (HL) was supplied. HL was then maintained for the rest of the experiment. In
1001 step 3, low nitrogen was supplied and high phosphate levels were restored (LNHP). In
1002 step 4, low phosphate was supplied and high nitrogen levels were restored (HNLP). In
1003 step 5, both nitrogen and phosphate were low (LNLP). Experimental steps were done
1004 in a consecutive manner. At each step, we measured cell concentration (**a**–**e**), medium
1005 pH_T value (**f**–**j**), medium pCO_2 level (**k**–**o**), dissolved inorganic nitrogen (DIN) (**p**–**t**)
1006 and phosphate (DIP) (**u**–**y**) concentrations in the media in the beginning and at the end
1007 of the incubations. Respectively, LC and HC represent pCO_2 levels of about 370 and
1008 960 μatm; LT and HT 16 and 20 ºC; LL and HL 60 and 240 μmol photons m^{-2} s^{-1} of
1009 photosynthetically active radiation (PAR); HN and LN 24.3 and 7.8 μmol L^{-1} NO_3^- at
1010 the beginning of the incubation; HP and LP 1.5 and 0.5 μmol L^{-1} PO_4^{3-} at the
1011 beginning of the incubations. The samples were taken in the last day of the cultures in
1012 each treatment. The values were indicated as the means ± sd of 4 replicate populations
1013 for each treatment.

1014

1015 **Figure 2.** Growth rate (**a**), particulate organic (POC, **b**) and inorganic (PIC, **c**) carbon
1016 quotas, PIC / POC value (**d**) and cell volume (**e**) of *Emiliania huxleyi* grown under the
1017 present (defined as low levels of pCO_2, temperature and light along with high levels
1018 of nutrients) and the future (defined as higher levels of pCO_2, temperature, and light

along with low levels of nutrients due to ocean acidification, warming and shoaling of upper mixing layer) scenarios. Data were obtained after cells were acclimated to experimental conditions for 14–16 generations and means ± sd of 4 replicate populations. Different letters (a, b) in each panel represent significant differences between future and present ocean conditions (Tukey Post hoc, $p < 0.05$).

Figure 3. Growth rates of *E. huxleyi* grown in LCLT (**a**), HCLT (**b**), LCHT (**c**) and HCHT (**d**) conditions, and the ratio of growth rate at HC to LC (**e**), HT to LT (**f**), HCHT to LCLT (**g**), LNHP to HNHP (**h**), HNLP to HNHP (**i**) and LNLP to HNHP (**j**). Data were obtained after cells were acclimated to experimental conditions for 14–16 generations and means ± sd of 4 replicate populations. Horizontal lines in panels (**e**)–(**j**) showed the value of 1. Different letters (a, b, c, d) in panels (**a**)–(**d**) represent significant differences between different nutrient treatments (Tukey Post hoc, $p < 0.05$). The results shown in the black column were used for the ambient-future comparison in figure 2. Detailed experimental conditions were shown in Figure 1.

Figure 4. POC quota of *E. huxleyi* grown in LCLT (**a**), HCLT (**b**), LCHT (**c**) and HCHT (**d**) conditions, and the ratio of POC quota at HC to LC (**e**), HT to LT (**f**), HCHT to LCLT (**g**), LNHP to HNHP (**h**), HNLP to HNHP (**i**) and LNLP to HNHP (**j**). Data were obtained after cells were acclimated to experimental conditions for 14–16 generations and means ± sd of 4 replicate populations. Horizontal lines in panels (**e**)–(**j**) showed the value of 1. Different letters (a, b) in panels (**a**)–(**d**) represent significant differences between different nutrient treatments (Tukey Post hoc, $p < 0.05$). The results shown in the black column were used for the ambient-future comparison in figure 2. Detailed experimental conditions were shown in Figure 1.

Figure 5. PIC quota of *E. huxleyi* grown in LCLT (**a**), HCLT (**b**), LCHT (**c**) and HCHT (**d**) conditions, and the ratio of PIC quota at HC to LC (**e**), HT to LT (**f**), HCHT to LCLT (**g**), LNHP to HNHP (**h**), HNLP to HNHP (**i**) and LNLP to HNHP (**j**). Data were obtained after cells were acclimated to experimental conditions for 14–16 generations and means ± sd of 4 replicate populations. Horizontal lines in panels (**e**)–(**j**) showed the value of 1. Different letters (a, b, c) in panels (**a**)–(**d**) represent significant differences between different nutrient treatments (Tukey Post hoc, $p < 0.05$). The results shown in the black column were used for the ambient-future comparison in figure 2. Detailed experimental conditions were shown in Figure 1.

Figure 6. PIC / POC value of *E. huxleyi* grown in LCLT (**a**), HCLT (**b**), LCHT (**c**) and HCHT (**d**) conditions, and the ratio of (PIC / POC value) at HC to LC (**e**), HT to LT (**f**), HCHT to LCLT (**g**), LNHP to HNHP (**h**), HNLP to HNHP (**i**) and LNLP to HNHP (**j**). Data were obtained after cells were acclimated to experimental conditions for 14–16 generations and means ± sd of 4 replicate populations. Horizontal lines in panels (**e**)–(**j**) showed the value of 1. Different letters (a, b, c) in panels (**a**)–(**d**) represent significant differences between different nutrient treatments (Tukey Post hoc, $p < 0.05$). The results shown in the black column were used for the ambient-future comparison in figure 2. Detailed experimental conditions were shown in Figure 1.

Figure S1. Flow chart of the experimental processes. Experimental steps were done in a consecutive manner. Detailed experimental conditions were shown in Figure 1.

Figure S2. Representative curves for the time course for cell concentrations of *E. huxleyi* under low pCO_2 (LC), high (HT) or low (LT) temperatures, and high light (HL) conditions with varying levels of nutrients: HNHP (**a**), LNHP (**b**), HNLP (**c**) and LNLP (**d**), respectively. Arrow indicates the day when samples were taken in each treatment. Data were means ± sd of 4 replicate populations. Detailed experimental conditions were shown in Figure 1.

Figure S3. Comparison of growth rate (**a**), POC quota (**b**) and PIC quota (**c**) between the expected (calculated) values and the measured values under the LNLP treatments. Different letters (a, b) in each "baseline" environment (LCLT, HCLT, LCHT or HCHT) represent significant differences (Tukey Post hoc, $p < 0.05$). Detailed experimental conditions were shown in Figure 1.

Figure S4. Heatmap of the changes in growth rate, POC quota, PIC quota and PIC:POC in each treatment. Values in the present scenario (LC LT LL HNHP) were considered as the control. A minus sign indicates the reduction in these parameters.

Figure S5. Cell volume of *E. huxleyi* grown in LCLT (**a**), HCLT (**b**), LCHT (**c**) and HCHT (**d**) conditions, and its correlation with POC quota (**e**) and PIC quota (**f**). Data were obtained after cells were acclimated to experimental conditions for 14–16 generations and means ± sd of 4 replicate populations in panels (**a**)–(**d**). Each point in panels (**e**) and (**f**) indicates an individual replicate from all experiment. Different letters (a, b, c) in panels (**a**)–(**d**) represent significant differences between different nutrient treatments (Tukey Post hoc, $p < 0.05$).

Figure S6. Normalized POC quota of *E. huxleyi* to cell volume in LCLT (**a**), HCLT (**b**), LCHT (**c**) and HCHT (**d**) conditions. Data were obtained after cells were acclimated to experimental conditions for 14–16 generations and means ± sd of 4 replicate populations. Different letters (a, b) in each panel represent significant differences between different nutrient treatments (Tukey Post hoc, $p < 0.05$).

Figure S7. Normalized PIC quota of *E. huxleyi* to cell volume in LCLT (**a**), HCLT (**b**), LCHT (**c**) and HCHT (**d**) conditions. Data were obtained after cells were acclimated to experimental conditions for 14–16 generations and means ± sd of 4 replicate populations. Different letters (a, b, c) in each panel represent significant differences between different nutrient treatments (Tukey Post hoc, $p < 0.05$).

Figure S8. POC production rate of *E. huxleyi* in LCLT (**a**), HCLT (**b**), LCHT (**c**) and HCHT (**d**) conditions, and the ratio of POC production rate at HC to LC (**e**), HT to LT (**f**), HCHT to LCLT (**g**), LNHP to HNHP (**h**), HNLP to HNHP (**i**) and LNLP to HNHP (**j**). Data were obtained after cells were acclimated to experimental conditions for 14–16 generations and means ± sd of 4 replicate populations. Horizontal lines in panels (**e**)–(**j**) showed the value of 1. Different letters (a, b, c) in panels (**a**)–(**d**) represent significant differences between different nutrient treatments (Tukey Post hoc, $p < 0.05$).

Figure S9. PIC production rate of *E. huxleyi* in LCLT (**a**), HCLT (**b**), LCHT (**c**) and HCHT (**d**) conditions, and the ratio of PIC production rate at HC to LC (**e**), HT to LT (**f**), HCHT to LCLT (**g**), LNHP to HNHP (**h**), HNLP to HNHP (**i**) and LNLP to HNHP (**j**). Data were obtained after cells were acclimated to experimental conditions

for 14–16 generations and means ± sd of 4 replicate populations. Horizontal lines in panels (**e**)–(**j**) showed the value of 1. Different letters (a, b, c) in panels (**a**)–(**d**) represent significant differences between different nutrient treatments (Tukey Post hoc, $p < 0.05$).

Figure S10. PON quota of *E. huxleyi* in LCLT (**a**), HCLT (**b**), LCHT (**c**) and HCHT (**d**) conditions, and the ratio of PON quota at HC to LC (**e**), HT to LT (**f**), HCHT to LCLT (**g**), LNHP to HNHP (**h**), HNLP to HNHP (**i**) and LNLP to HNHP (**j**). Data were obtained after cells were acclimated to experimental conditions for 14–16 generations and means ± sd of 4 replicate populations. Horizontal lines in panels (**e**)–(**j**) showed the value of 1. Different letters (a, b) in panels (**a**)–(**d**) represent significant differences between different nutrient treatments (Tukey Post hoc, $p < 0.05$).

Figure S11. Normalized RNA quota of *E. huxleyi* to POC quota in HNHP and HNLP conditions. Data were obtained after cells were acclimated to experimental conditions for 14–16 generations and means ± sd of 4 replicate populations. Different letters (a, b) represent significant differences between different nutrient treatments (Tukey Post hoc, $p < 0.05$).

Table 1. Carbonate chemistry parameters at the end of the incubation. The values are means ± sd of 4 replicate populations. LL and HL represent 60 and 240 µmol photons m^{-2} s^{-1} of photosynthetically active radiation (PAR), respectively; HN and LN represent 24.3 and 7.8 µmol L^{-1} DIN in the beginning of the incubation; HP and LP represent 1.5 and 0.5 µmol L^{-1} DIP in the beginning of the incubation, respectively.

			pCO_2 (µatm)	pH (total scale)	TA (µmol L^{-1})	DIC (µmol L^{-1})	HCO_3^- (µmol L^{-1})	CO_3^{2-} (µmol L^{-1})	CO_2 (µmol L^{-1})
16	LL-HNHP	LC	371±17	8.07±0.02	2266±19	2017±9	1823±6	180±8	13.4±0.6
		HC	918±21	7.73±0.02	2248±45	2149±39	2027±35	90±5	33.3±0.7
	HL-HNHP	LC	387±22	8.06±0.02	2297±12	2050±17	1857±20	179±6	14.0±0.8
		HC	972±11	7.71±0.01	2283±34	2189±31	2066±29	88±3	35.2±0.4
	HL-LNHP	LC	393±20	8.05±0.02	2273±9	2033±3	1845±9	174±7	14.3±0.7
		HC	1012±13	7.69±0.01	2263±28	2177±25	2057±24	84±2	36.7±0.5
	HL-HNLP	LC	395±19	8.06±0.02	2318±5	2073±12	1879±16	179±6	14.3±0.7
		HC	958±63	7.70±0.01	2205±69	2117±71	1999±69	84±1	34.7±2.3
	HL-LNLP	LC	375±24	8.06±0.01	2181±78	1947±77	1767±73	167±3	13.6±0.9
		HC	1014±46	7.68±0.01	2198±73	2118±73	2002±69	79±2	36.7±1.7
20	LL-HNHP	LC	349±16	8.09±0.02	2257±14	1963±4	1741±6	210±8	11.3±0.5
		HC	899±40	7.74±0.02	2257±53	2130±45	1994±40	107±7	29.0±1.3
	HL-HNHP	LC	363±11	8.08±0.01	2281±16	1990±18	1770±19	208±2	11.7±0.3
		HC	947±24	7.72±0.01	2248±21	2130±19	1998±18	102±3	30.6±0.8
	HL-LNHP	LC	362±18	8.08±0.02	2262±12	1973±13	1756±16	206±7	11.7±0.6
		HC	970±10	7.71±0.01	2271±31	2155±28	2021±25	102±3	31.4±0.3
	HL-HNLP	LC	370±14	8.08±0.01	2314±3	2023±10	1800±14	211±4	12.0±0.4
		HC	946±47	7.71±0.01	2200±72	2088±72	1960±68	98±2	30.6±1.5
	HL-LNLP	LC	350±18	8.08±0.01	2193±71	1912±68	1701±63	200±5	11.3±0.6
		HC	977±59	7.70±0.01	2192±78	2086±79	1959±76	95±2	31.6±1.9

Table 2. Final nitrate and phosphate concentrations (N : P, μmol L^{-1}), growth rate (d^{-1}), POC and PIC quotas (pg C $cell^{-1}$), and PIC / POC value. Values in the brackets represent final DIN and DIP concentrations, and standard deviation of 4 replicate populations for growth rate, POC and PIC quotas, and PIC / POC value. Detailed information was shown in Table 1.

pCO_2	T	Light	Final N : P	Growth rate	POC quota	PIC quota	PIC/POC
LC	LT	LL	HNHP (17.1 : 0.7)	0.96 (0.012)	1.80 (0.14)	0.38 (0.09)	0.21 (0.07)
		HL	HNHP (17.3 : 0.5)	1.09 (0.006)	2.50 (0.28)	0.62 (0.05)	0.25 (0.05)
		HL	LNHP (2.5 : 0.6)	1.00 (0.013)	2.07 (0.25)	0.90 (0.02)	0.44 (0.05)
		HL	HNLP (15.4 : 0.1)	1.08 (0.006)	2.42 (0.08)	0.83 (0.04)	0.34 (0.01)
		HL	LNLP (2.4 : 0.1)	0.99 (0.003)	2.62 (0.25)	1.62 (0.14)	0.63 (0.11)
HC	LT	LL	HNHP (18.6 : 0.9)	0.79 (0.012)	2.52 (0.33)	0.26 (0.06)	0.10 (0.04)
		HL	HNHP (18.2 : 0.5)	1.04 (0.012)	2.85 (0.36)	0.41 (0.06)	0.15 (0.04)
		HL	LNHP (2.0 : 0.6)	0.92 (0.026)	2.75 (0.23)	0.68 (0.03)	0.25 (0.03)
		HL	HNLP (15.5 : 0.1)	0.85 (0.002)	5.06 (0.34)	0.64 (0.05)	0.13 (0.01)
		HL	LNLP (2.7 : 0.1)	0.67 (0.005)	4.91 (0.28)	0.90 (0.01)	0.18 (0.01)
LC	HT	LL	HNHP (16.6 : 0.3)	1.03 (0.006)	1.58 (0.11)	0.43 (0.02)	0.27 (0.01)
		HL	HNHP (17.3 : 0.3)	1.46 (0.004)	2.15 (0.28)	0.52 (0.07)	0.25 (0.06)
		HL	LNHP (2.1 : 0.5)	1.42 (0.004)	1.68 (0.05)	0.79 (0.04)	0.47 (0.03)
		HL	HNLP (17.0 : 0.1)	1.44 (0.004)	2.09 (0.03)	1.00 (0.05)	0.48 (0.03)
		HL	LNLP (2.1 : 0.1)	1.39 (0.038)	2.02 (0.05)	1.17 (0.13)	0.58 (0.07)
HC	HT	LL	HNHP (16.7 : 0.4)	0.99 (0.008)	1.54 (0.12)	0.34 (0.05)	0.22 (0.04)
		HL	HNHP (17.9 : 0.5)	1.43 (0.001)	2.57 (0.06)	0.42 (0.02)	0.16 (0.01)
		HL	LNHP (2.4 : 0.6)	1.38 (0.009)	1.97 (0.03)	0.52 (0.03)	0.27 (0.01)
		HL	HNLP (17.1 : 0.1)	1.27 (0.018)	3.68 (0.50)	0.74 (0.06)	0.20 (0.02)
		HL	LNLP (2.2 : 0.1)	0.87 (0.022)	3.81 (0.39)	0.89 (0.10)	0.20 (0.04)

Table 3. Results of three-way ANOVAs of the effects of temperature (T), pCO_2 (C) and light intensity (L) and their interaction on growth rate, POC and PIC quotas, and PIC / POC value. Significant values were marked in bold.

		T	C	L	T×C	T×L	C×L	T×C×L
Growth rate	F	20037.5	477.4	23625.8	120.0	1550.9	34.0	86.4
	p	**<0.01**	**<0.01**	**<0.01**	**<0.01**	**<0.01**	**<0.01**	**<0.01**
POC quota	F	27.1	54.4	62.0	7.4	1.9	< 0.1	6.1
	p	**<0.01**	**<0.01**	**<0.01**	**0.01**	0.18	0.83	**0.02**
PIC quota	F	0.4	38.6	47.6	2.3	6.6	1.6	1.1
	p	0.56	**<0.01**	**<0.01**	0.14	**0.02**	0.22	0.31
PIC / POC value	F	9.9	443.6	2.0	0.8	10.0	0.6	0.3
	p	**<0.01**	**<0.01**	0.17	0.38	**<0.01**	0.46	0.60

Table 4. Results of four-way ANOVAs of the effects of temperature (T), pCO_2 (C), dissolved inorganic nitrate (N) and phosphate (P) concentrations and their interaction on growth rate, POC and PIC quotas, and PIC / POC value. Significant values were marked in bold.

	Growth rate		POC quota		PIC quota		PIC / POC value	
	F	*p*	F	*p*	F	*p*	F	*p*
T	500026.0	**<0.01**	297.4	**<0.01**	30.2	**<0.01**	82.8	**<0.01**
C	5798.0	**<0.01**	162.8	**<0.01**	376.2	**<0.01**	787.3	**<0.01**
N	4542.0	**<0.01**	157.0	**<0.01**	84.4	**<0.01**	127.6	**<0.01**
P	5347.0	**<0.01**	206.5	**<0.01**	474.6	**<0.01**	0.1	0.74
T×C	6899.0	**<0.01**	52.2	**<0.01**	0.2	0.68	7.2	**<0.01**
T×N	510.0	**<0.01**	5.6	**0.02**	60.0	**<0.01**	7.9	**<0.01**
T×P	39.0	**<0.01**	5.2	**0.03**	9.4	**<0.01**	16.2	**<0.01**
C×N	1265.0	**<0.01**	107.2	**<0.01**	9.5	**<0.01**	3.1	0.09
C×P	1718.0	**<0.01**	174.1	**<0.01**	14.7	**<0.01**	88.0	**<0.01**
N×P	179.0	**<0.01**	19.7	**<0.01**	10.7	**<0.01**	14.3	**<0.01**
T×C×N	35.0	**<0.01**	<0.1	0.81	0.2	0.67	1.9	0.17
T×C×P	27.0	**<0.01**	5.5	**0.02**	0.1	0.71	1.0	0.31
T×N×P	96.0	**<0.01**	<0.1	0.80	15.7	**<0.01**	3.3	0.08
C×N×P	241.0	**<0.01**	0.4	0.56	8.2	**<0.01**	1.2	0.28
T×C×N×P	105.0	**<0.01**	3.9	0.05	22.4	**<0.01**	4.5	**0.04**

Table 5. List of the physiological responses of *E. huxleyi* to the concurrent changes in multiple drivers investigated by the laboratory incubations in the published studies. '↑' represents increase, '↓' represents decrease, and 'n' represents no significant change to simultaneous changes in multiple drivers. C, T, L, N, P and μ represent CO_2 (μatm), temperature (°C), light intensity (μmol photons m^{-2} s^{-1}), dissolved inorganic nitrogen and phosphate (μmol L^{-1}), and growth rate, respectively. Simultaneous changes in multiple drivers were marked in bold. [1] represents De Bodt et al., (2010), [2] Borchard et al., (2011), [3] Sett et al., (2014), [4] Gafar and Schulz, (2018), [5] Tong et al., (2019), [6] Jin et al., (2017), [7] Bretherton et al., (2019), [8] Rost et al., (2002), [9] Feng et al., (2008), [10] Müller et al., (2012), [11] Perrin et al., (2016), [12] Leonardos and Geider, (2005), [13] Matthiessen et al., (2012), [14] Zhang et al., (2019), [15] this study.

Strain	C	T	L	N	P	μ	POC	PIC	PIC: POC	Cite
AC481	**380 to 750**	**13 to 18**	150	32	1	n	↑	↓	↓	[1]
PML B92/11	**300 to 900**	**14 to 18**	300	29	1	↑	n	↓	↓	[2]
PML B92/11	**400 to 1000**	**10 to 20**	150	64	4	↑	↑	↓	↓	[3]
PML B92/11	**400 to 1000**	**10 to 20**	150	64	4	↑	↓	↓		[4]
PML B92/11	**400 to 1000**	**15 to 24**	190	100	10	↑	↑	↓	↓	[5]
CCMP2090	**395 to 1000**	20	**57 to 567**	110	10	↑	↑			[6]
NZEH	**390 to 1000**	20	**175 to 300**	100	10	↓	↑	↑	↑	[7]
PCC124-3	**390 to 1000**	20	**175 to 300**	100	10	↑	n	↑	↑	[7]
PCC70-3	**390 to 1000**	20	**175 to 300**	100	10	↑	n	↑	↑	[7]
PML B92/11	**140 to 880**	15	**80 to 150**	100	6	↑	↑	↓	↓	[8]
PML B92/11	**395 to 1000**	20	**54 to 457**	110	10	↑	↑	↓	↓	[6]
PML B92/11	**400 to 1000**	20	**50 to 1200**	64	4	↑	↑	↑		[4]
RCC962	**390 to 1000**	20	**175 to 300**	100	10	↓	↑	n	↓	[7]
CCMP371	**375 to 750**	**20 to 24**	**50 to 400**	100	10	↑	n	↓	↓	[9]
B62	**280 to 1000**	20	300	**88 to 9**	4		↑	↓	↓	[10]
RCC911	400	20	**30 to 140**	**100 to 5**	6	↑	↑	↑	↑	[11]
RCC911	400	20	**30 to 140**	100	**6 to 0.6**	↑	↑	↑	↑	[11]

PML92A	**360 to 2000**	18	**80 to 500**	200	**6.7 to 40**	n	↑			[12]
A	**460 to 1280**	16	130	**17 to 9**	**0.2 to 0.5**		↓	↓		[13]
PML B92/11	**410 to 920**	20	**80 to 480**	**100 to 8**	10	↓	↓	↑	↑	[14]
PML B92/11	**410 to 920**	20	**80 to 480**	100	**10 to 0.4**	↓	↑	n	↓	[14]
PML B92/11	**370 to 960**	**16 to 20**	**60 to 240**	**24 to 8**	**1.5 to 0.5**	↓	↑	↑	n	[15]

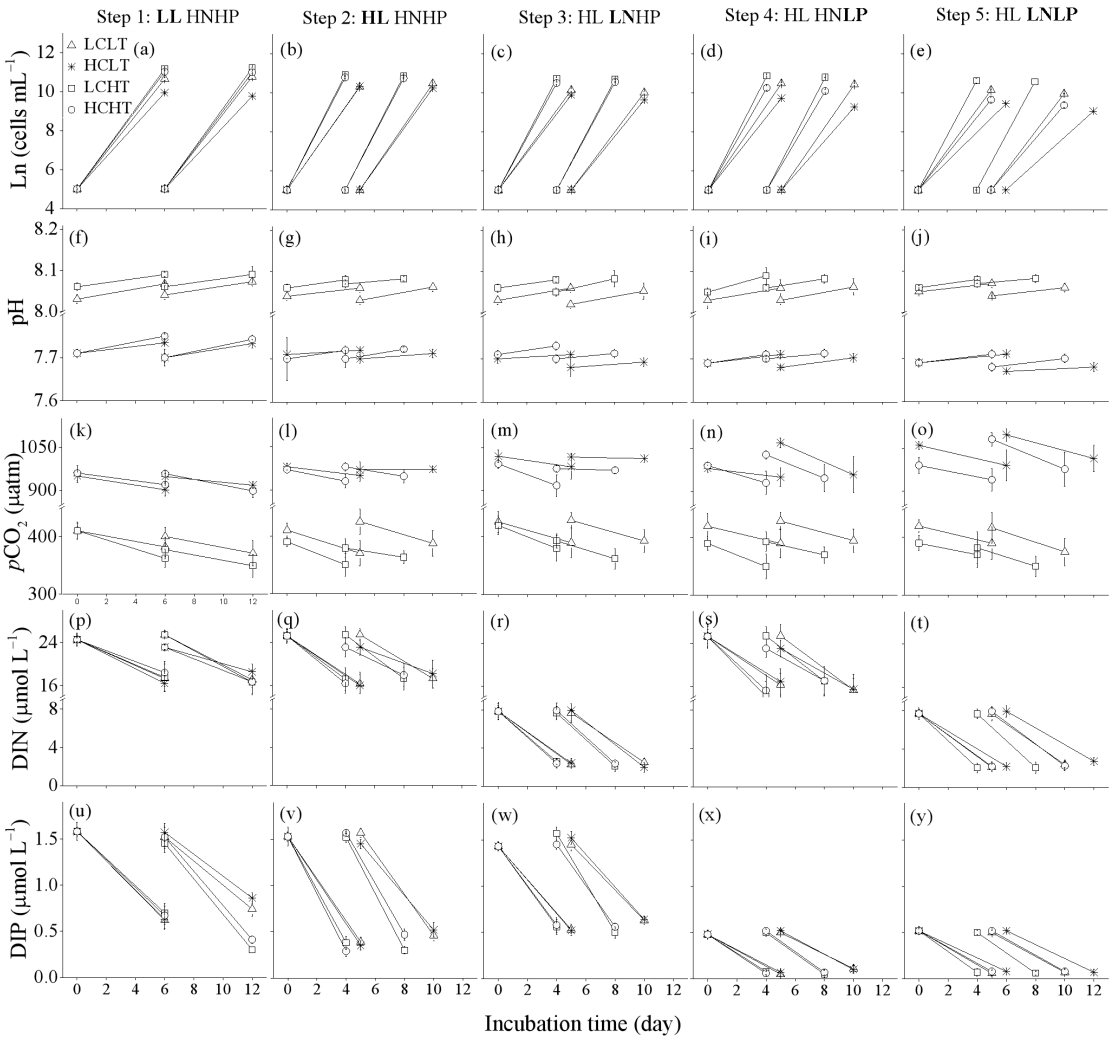
Step 1: LL HNHP
Step 2: HL HNHP
Step 3: HL LNHP
Step 4: HL HNLP
Step 5: HL LNLP
LCLT
HCLT
LCHT
HCHT
Ln (cells mL^{-1})
pH
pCO_2 (µatm)
DIN (µmol L^{-1})
DIP (µmol L^{-1})
Incubation time (day)

Figure 1

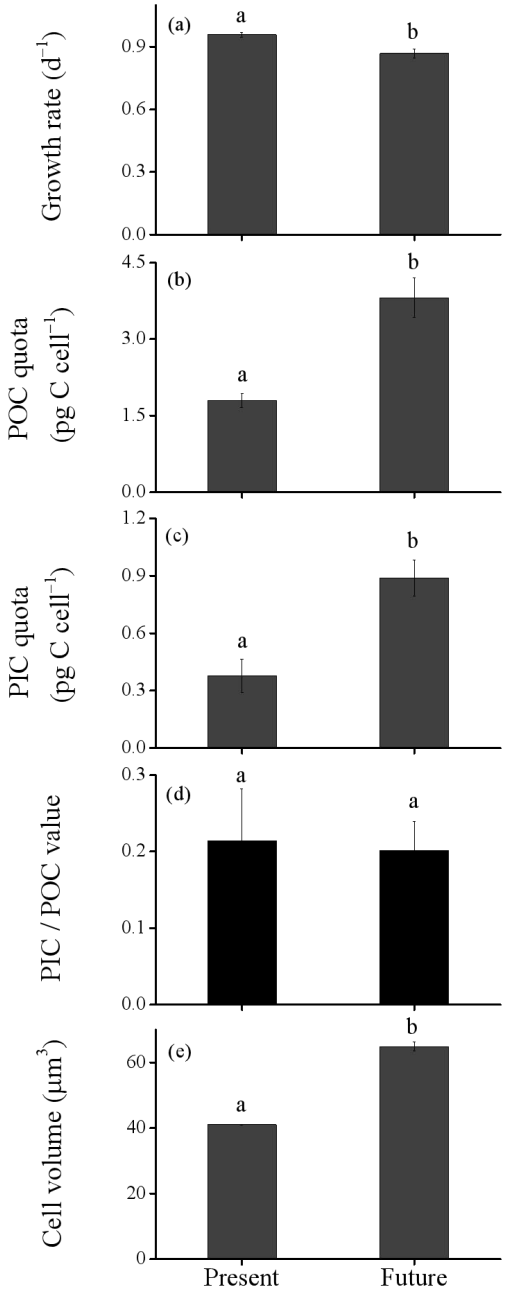
(a)
Growth rate (d^{-1})
0.0
0.3
0.6
0.9
a
b
(b)
POC quota (pg C cell^{-1})
0.0
1.5
3.0
4.5
a
b
(c)
PIC quota (pg C cell^{-1})
0.0
0.3
0.6
0.9
1.2
a
b
(d)
PIC / POC value
0.0
0.1
0.2
0.3
a
a
(e)
Cell volume (μm^3)
0
20
40
60
a
b
Present
Future

Figure 2

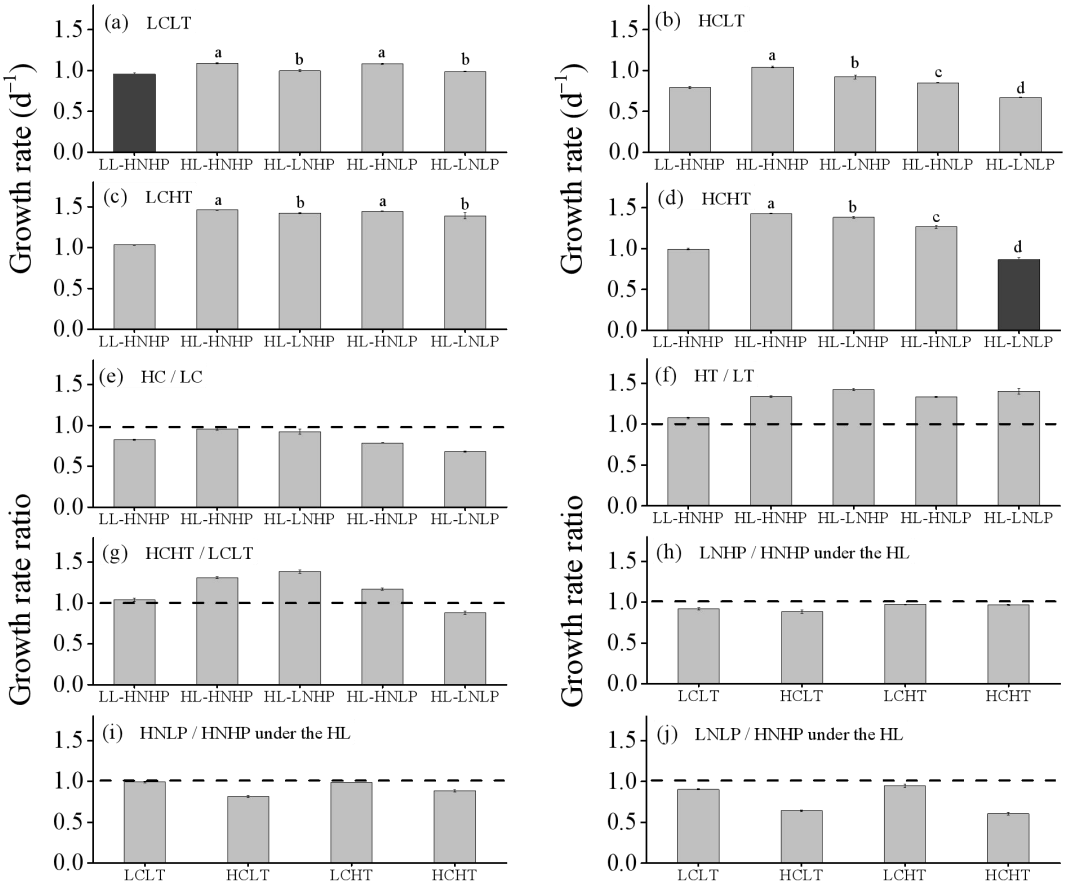
(a) LCLT
(b) HCLT
(c) LCHT
(d) HCHT
(e) HC / LC
(f) HT / LT
(g) HCHT / LCLT
(h) LNHP / HNHP under the HL
(i) HNLP / HNHP under the HL
(j) LNLP / HNHP under the HL
Growth rate (d^{-1})
Growth rate ratio
LL-HNHP
HL-HNHP
HL-LNHP
HL-HNLP
HL-LNLP
LCLT
HCLT
LCHT
HCHT

Figure 3

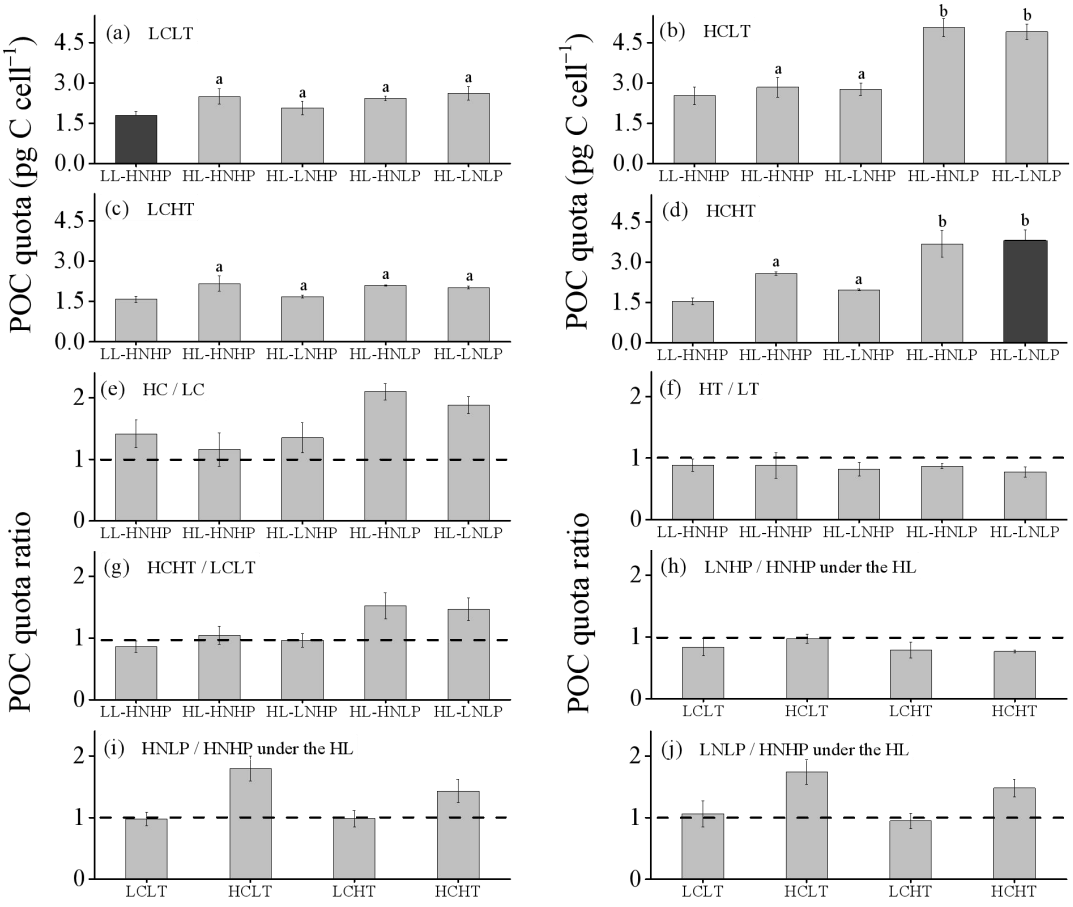
(a) LCLT
(b) HCLT
(c) LCHT
(d) HCHT
(e) HC / LC
(f) HT / LT
(g) HCHT / LCLT
(h) LNHP / HNHP under the HL
(i) HNLP / HNHP under the HL
(j) LNLP / HNHP under the HL
POC quota (pg C cell^{-1})
POC quota ratio
LL-HNHP
HL-HNHP
HL-LNHP
HL-HNLP
HL-LNLP
LCLT
HCLT
LCHT
HCHT

Figure 4

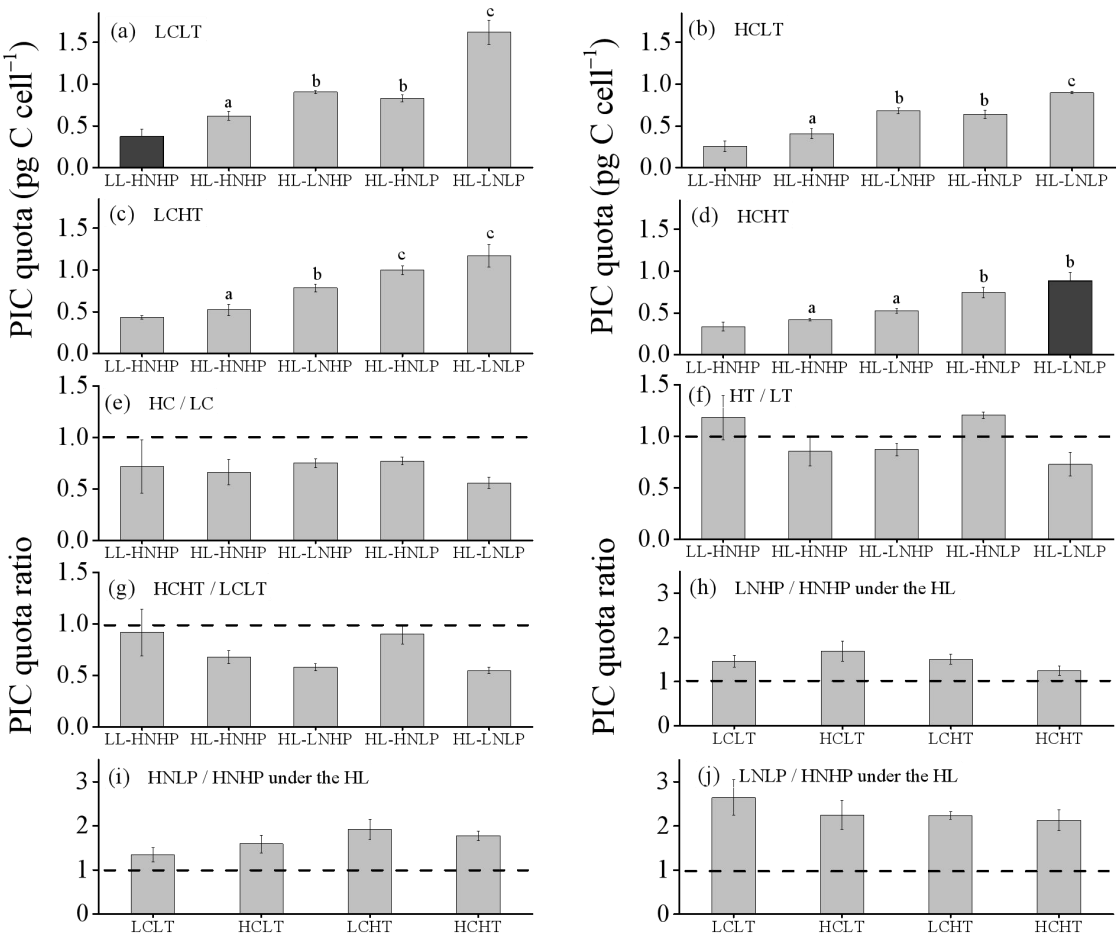
(a) LCLT
(b) HCLT
(c) LCHT
(d) HCHT
(e) HC / LC
(f) HT / LT
(g) HCHT / LCLT
(h) LNHP / HNHP under the HL
(i) HNLP / HNHP under the HL
(j) LNLP / HNHP under the HL
PIC quota (pg C cell^{-1})
PIC quota ratio
LL-HNHP
HL-HNHP
HL-LNHP
HL-HNLP
HL-LNLP
LCLT
HCLT
LCHT
HCHT

Figure 5

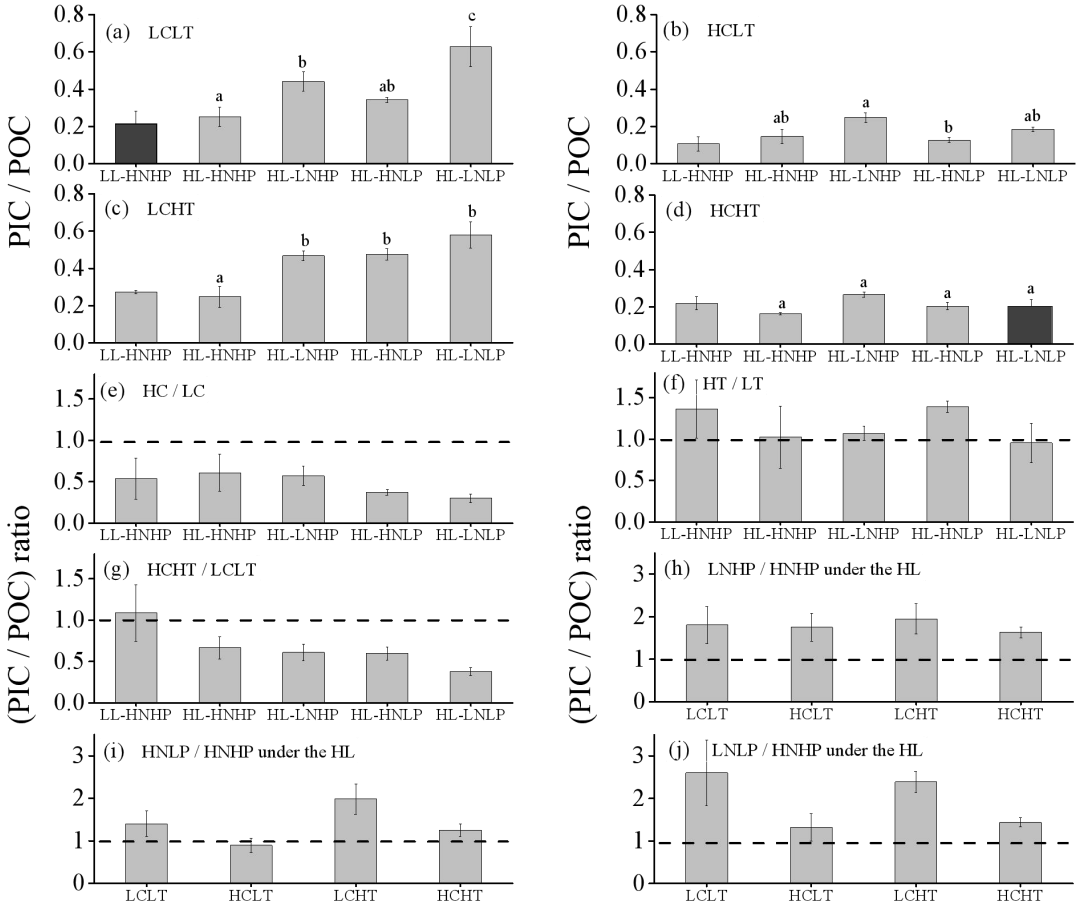
PIC / POC
(PIC / POC) ratio
(a) LCLT
(b) HCLT
(c) LCHT
(d) HCHT
(e) HC / LC
(f) HT / LT
(g) HCHT / LCLT
(h) LNHP / HNHP under the HL
(i) HNLP / HNHP under the HL
(j) LNLP / HNHP under the HL
LL-HNHP
HL-HNHP
HL-LNHP
HL-HNLP
HL-LNLP
LCLT
HCLT
LCHT
HCHT

Figure 6